

AD-A058 366

PROTOTYPE DEVELOPMENT ASSOCIATES INC SANTA ANA CALIF
MULTI-RAY ABLATION SENSOR DEVELOPMENT PROGRAM. (U)
APR 77 H L MOODY

F/G 18/4

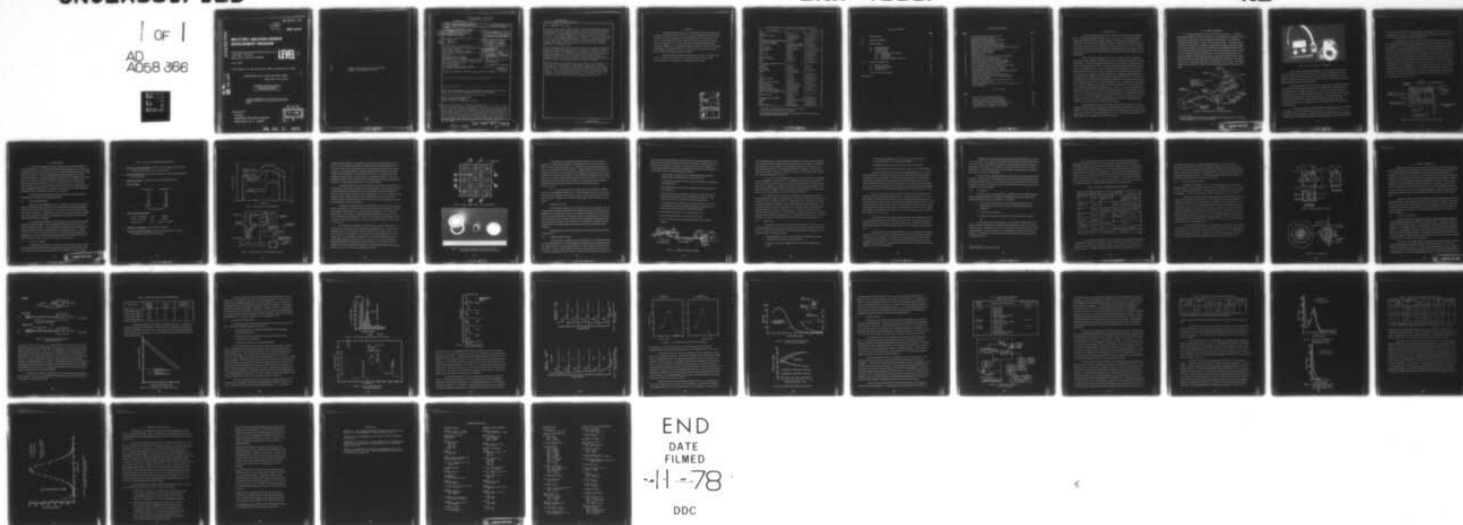
DNA001-75-C-0315

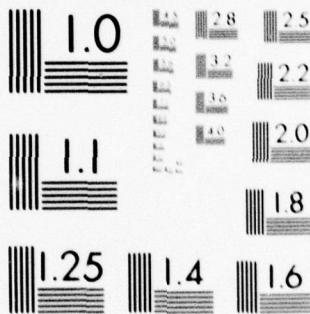
UNCLASSIFIED

DNA-4533F

NL

1 of 1
AD
A058 366





MICROCOPY RESOLUTION TEST CHART

AD-E300 281

12

DNA 4533F

ADA 058366

MULTI-RAY ABLATION SENSOR DEVELOPMENT PROGRAM

Prototype Development Associates, Inc.
1740 Garry Avenue
Santa Ana, California 92705

LEVEL II

April 1977

Final Report for Period 2 June 1975—15 December 1976

CONTRACT Nos. DNA 001-75-C-0315
DNA 001-76-C-0140

APPROVED FOR PUBLIC RELEASE;
DISTRIBUTION UNLIMITED.

THIS WORK SPONSORED BY THE DEFENSE NUCLEAR AGENCY
UNDER RDT&E RMSS CODE X342075469 Q93QAXAD41025/26/27/31
H2590D.

Prepared for
Director
DEFENSE NUCLEAR AGENCY
Washington, D. C. 20305

DDC
RECEIVED
SEP 5 1978
B

78 06 21 001

AJ NO. _____
DDC FILE COPY

Destroy this report when it is no longer
needed. Do not return to sender.



UNCLASSIFIED

SECURITY CLASSIFICATION OF THIS PAGE (When Data Entered)

19 REPORT DOCUMENTATION PAGE		READ INSTRUCTIONS BEFORE COMPLETING FORM
1. REPORT NUMBER	2. GOVT ACCESSION NO.	3. RECIPIENT'S CATALOG NUMBER
DNA 4533F; AD-E300 281		
4. TITLE (and Subtitle)	5. TYPE OF REPORT & PERIOD COVERED	6. PERFORMING ORG. REPORT NUMBER
MULTI-RAY ABLATION SENSOR DEVELOPMENT PROGRAM.	Final Report for Period 2 Jun 75-15 Dec 76.	
7. AUTHOR(s)	8. CONTRACT OR GRANT NUMBER(s)	
H. L./Moody	DNA 001-75-C-0315 DNA 001-76-C-0140	
9. PERFORMING ORGANIZATION NAME AND ADDRESS	10. PROGRAM ELEMENT, PROJECT, TASK AREA & WORK UNIT NUMBERS	
Prototype Development Associates, Inc. 1740 Garry Avenue Santa Ana, California 92705	NWED Subtask Q93QAXAD410-25/26/27/31	
11. CONTROLLING OFFICE NAME AND ADDRESS	12. REPORT DATE	13. NUMBER OF PAGES
Director Defense Nuclear Agency Washington, D.C. 20305	April 1977	48
14. MONITORING AGENCY NAME & ADDRESS (if different from Controlling Office)	15. SECURITY CLASS (of this report)	15a. DECLASSIFICATION/DOWNGRADING SCHEDULE
Space and Missile Systems Organization Worldway Postal Center P. O. Box 92960 Los Angeles, California 90009	UNCLASSIFIED	
16. DISTRIBUTION STATEMENT (of this Report)		
Approved for public release; distribution unlimited.		
17. DISTRIBUTION STATEMENT (of the abstract entered in Block 20, if different from Report)		
18. SUPPLEMENTARY NOTES		
This work sponsored by the Defense Nuclear Agency under RDT&E RMSS Code X342075469 Q93QAXAD41025/26/27/31 H2590D.		
19. KEY WORDS (Continue on reverse side if necessary and identify by block number)		
Nosetip Ablation Measurement Shape Change Measurement Multiple Channel Gamma-Ray Detector		
20. ABSTRACT (Continue on reverse side if necessary and identify by block number)		
This report documents the design analyses and test results that were performed in the development of a Multi-Ray Ablation Sensor. The sensor was designed to measure nosetip ablation along nine individual rays with a single photon counting tube (Digicon tube). The sensor measures ablation by measuring the change in gamma- ray activity of radioactive sources located in the nosetip. Nine CsI scintillators convert the incident gamma-rays into photons (light) which are coupled to the photon counting tube with		

DD FORM 1 JAN 73 1473A EDITION OF 1 NOV 65 IS OBSOLETE

UNCLASSIFIED

SECURITY CLASSIFICATION OF THIS PAGE (When Data Entered)

390 714

78 06 21 001
LB

UNCLASSIFIED

SECURITY CLASSIFICATION OF THIS PAGE(When Data Entered)

20. ABSTRACT (Continued)

flexible fiber optic light guides. The light guides are positioned on the Digicon tube's photocathode so that the photoelectrons generated by light guide photons are electrostatically focused to a corresponding diode on the anode end of the tube. The nine light guide images on the photocathode are focused, one-to-one, on a corresponding array of diodes. The photoelectrons are accelerated and focused with -15 kV and an electrostatic lens. The signal outputs from the diodes are amplified and shaped for input into conventional reentry vehicle telemetry interface electronics. ✕

Three prototype Multi-Ray Ablation Sensors were fabricated and tested to determine the sensor's electrical and nuclear performance and their performance under vibration. The tests show that the sensors are inherently low-noise and highly efficient multiple gamma-ray counters with excellent gain stability. Random vibration tests at $0.8 \text{ g}^2/\text{Hz}$ show that the sensor is unaffected by vibration provided a vibration isolation system is used to support the Digicon tube-amplifier assembly.

The Multi-Ray Ablation Sensor is concluded to be efficient in both nuclear and electrical performance and offers extreme flexibility in packaging. The sensor electronics can be separated from the vibration-insensitive scintillators with fiber optics. This allows extreme flexibility in collimator design because of the miniature scintillation detectors. Also, the electronics can be packaged in areas of the vehicle with low vibration inputs and/or greater packaging flexibility.

UNCLASSIFIED

SECURITY CLASSIFICATION OF THIS PAGE(When Data Entered)

PREFACE

The studies described in this report were performed by Prototype Development Associates, Inc. (PDA), Santa Ana, California, and Science Applications, Inc. (SAI), under subcontract to PDA, for the Defense Nuclear Agency (DNA) under Contract Numbers DNA 001-75-C-0315 and DNA 001-76-C-0140. Major T. W. Swartz was the DNA Contracting Officer's Representative. The work was sponsored by the Space and Missile Systems Organization (SAMSO), Air Force Systems Command, Los Angeles, California. The SAMSO Project Officer was Captain M. Elliott. Dr. S. Brelant of The Aerospace Corporation served as the principal technical monitor for SAMSO.

The technical effort was performed under the direction of H. L. Moody of PDA and Dr. V. Orphan of SAI. Significant contributions to the effort were provided by Dr. R. Ginaven, Dr. V. Verbinski, Mr. J. Brayors and Mr. E. Julian.

ACCESSION		
NTIS	DATA SECTION	<input checked="" type="checkbox"/>
DDC	DATA SECTION	<input type="checkbox"/>
UNANIMOUS		<input type="checkbox"/>
JUSTIFICATION		
BY		
DISTRIBUTION/AVAILABILITY CODES		
Dist.	AVAIL.	and/or SPECIAL
A		

Conversion factors for U. S. customary to metric (SI) units of measurement.

To Convert From	To	Multiply By
angstrom	meters (m)	1.000 000 X E -10
atmosphere (normal)	kilo pascal (kPa)	1.013 25 X E +2
bar	kilo pascal (kPa)	1.000 000 X E +2
barn	meter ² (m ²)	1.000 000 X E -28
British thermal unit (thermochemical)	joule (J)	1.054 350 X E +3
calorie (thermochemical)	joule (J)	4.184 000
cal (thermochemical)/cm ²	mega joule/m ² (MJ/m ²)	4.184 000 X E -2
curie	giga becquerel (GBq)*	3.700 000 X E +1
degree (angle)	radian (rad)	1.745 329 X E -2
degree Fahrenheit	degree kelvin (K)	$T_K = (t^{\circ}F + 459.67)/1.8$
electron volt	joule (J)	1.602 19 X E -19
erg	joule (J)	1.000 000 X E -7
erg/second	watt (W)	1.000 000 X E -7
foot	meter (m)	3.048 000 X E -1
foot-pound-force	joule (J)	1.355 818
gallon (U. S. liquid)	meter ³ (m ³)	3.785 412 X E -3
inch	meter (m)	2.540 000 X E -2
jerk	joule (J)	1.000 000 X E +9
joule/kilogram (J/kg) (radiation dose absorbed)	Gray (Gy)**	1.000 000
kilotons	terajoules	4.183
kip (1000 lbf)	newton (N)	4.448 222 X E +3
kip/inch ² (ksi)	kilo pascal (kPa)	6.894 757 X E +3
ktap	newton-second/m ² (N-s/m ²)	1.000 000 X E +2
micron	meter (m)	1.000 000 X E -6
mil	meter (m)	2.540 000 X E -5
mile (international)	meter (m)	1.609 344 X E +3
ounce	kilogram (kg)	2.834 952 X E -2
pound-force (lbf avoirdupois)	newton (N)	4.448 222
pound-force inch	newton-meter (N·m)	1.129 848 X E -1
pound-force/inch	newton/meter (N/m)	1.751 268 X E +2
pound-force/foot ²	kilo pascal (kPa)	4.788 026 X E -2
pound-force/inch ² (psi)	kilo pascal (kPa)	6.894 757
pound-mass (lbm avoirdupois)	kilogram (kg)	4.535 924 X E -1
pound-mass-foot ² (moment of inertia)	kilogram-meter ² (kg·m ²)	4.214 011 X E -2
pound-mass/foot ³	kilogram/meter ³ (kg/m ³)	1.601 846 X E +1
rad (radiation dose absorbed)	Gray (Gy)**	1.000 000 X E -2
roentgen	coulomb/kilogram (C/kg)	2.579 760 X E -4
shake	second (s)	1.000 000 X E -8
slug	kilogram (kg)	1.459 390 X E +1
torr (mm Hg, 0° C)	kilo pascal (kPa)	1.333 22 X E -1

*The becquerel (Bq) is the SI unit of radioactivity; 1 Bq = 1 event/s.

**The Gray (Gy) is the SI unit of absorbed radiation.

A more complete listing of conversions may be found in "Metric Practice Guide E 380-74," American Society for Testing and Materials.

TABLE OF CONTENTS

	<u>Page</u>
1.0 INTRODUCTION	5
2.0 SENSOR DESCRIPTION	7
3.0 SENSOR DESIGN	11
3.1 Design Requirements	11
3.2 Electrical Design	11
3.3 Mechanical Design	16
3.3.1 Scintillator/Optical Coupling	16
3.3.2 Digicon Tube	18
3.3.3 Preamplifiers	20
3.3.4 High Voltage Supply and Gas Seal	22
4.0 SENSOR PERFORMANCE	25
4.1 Optical Performance	25
4.2 Electrical Performance	28
4.3 Vibration Tests	34
5.0 SUMMARY AND CONCLUSIONS	41
REFERENCES	43

LIST OF ILLUSTRATIONS

<u>Figure</u>		<u>Page</u>
1	Nine-Channel Multi-Ray Sensor Schematic	7
2	Nine-Channel Sensor Components	8
3	Schematic of 9-Channel Digicon and Amplifiers	9
4	Multi-Ray Vibration Specifications	13
5	Multi-Ray Sensor Vehicle Electrical Schematic	13
6	Header Design for Nine-Channel Digicon Tube	15
7	Nine-Channel Digicon Tube Components (Tube Body, Electrostatic Focus Cone, and Nine-Diode Array Header)	15
8	Scintillator and Optical Coupling	17
9	Multi-Ray Detector Container	23
10	Fiber Optical Seal	23
11	Transmission Measurements for Fiber Optic Light Guide	26
12	Transmissivity of Candidate Fiber Optics	27
13	Typical Pulse Height Distribution from the Digicon	29
14	Four-Channel Digicon Tube Pulse Height Distribution	29
15	Effect of Tube Voltage on Pulse Height Spectrum	30
16	Effect of Amplifier Shaping Time Constant on Pulse Height	31
17	Effect of Diode Bias Voltage on Pulse Height	31
18	Nine-Channel Digicon Pulse Height Distributions	32
19	Response of Digicon Tube to Scan Across Fiber Optic Magnifier	33
20	Measured Nuclear Efficiencies of Sensor	33
21	Typical Sensor Vibration Test Electrical Schematic	35
22	Sensor S/N 351 Vibration Test Pulse Height Distributions (Voltage Applied to Tube)	38
23	Sensor S/N 351 Vibration Test Pulse Height Distributions (No Voltage Applied to Tube)	38
24	Pulse Height Distribution Comparison Pretest and During $0.8 \text{ g}^2/\text{Hz}$ Random Vibration	40

LIST OF TABLES

<u>Table</u>		<u>Page</u>
1	Sensor Environmental Design Requirements	12
2	Summary of Preamplifier Development Effort	21
3	Fiber Optic Cable Transmission Measurements	27
4	Sensor Hardware Subjected to Random Vibration Tests	35
5	Digicon Tube S/N 352 Vibration Test Count Rate	37
6	Digicon Tube S/N 351 Vibration Test Count Rate	39

1.0 INTRODUCTION

A Multi-Ray Ablation Sensor has been developed for measuring nosetip and, if applicable, heatshield ablation along nine individual rays. The sensor uses a compact digital photon-counting tube (Digicon tube) that is capable of measuring, simultaneously, ablation along nine individual rays. The sensor and associated electronics were designed and fabricated for potential use on reentry vehicles under contracts DNA001-75-C-0315 and DNA001-76-C-0140. The sensor has undergone electrical, nuclear and simulated reentry vibration testing for the purpose of evaluating sensor performance under simulated reentry environments and in typical nosetip and vehicle configurations.

The sensor has been developed in three phases. In Phase I, the basic feasibility of using Digicon tubes for multiple ray ablation sensors was investigated and the results are described in Reference 1. In Phase I, the Multi-Ray Ablation Sensor was mocked up in the laboratory and nuclear detection efficiency (for ^{182}Ta), cross talk, background and ablation sensitivity were determined in a preliminary fashion. Phase II involved the design and development of a nine channel ablation sensor for use on reentry vehicles. This phase was funded under contract DNA001-75-C-0315 and involved 1) designing a nine-channel Digicon tube, 2) developing optical coupling between the Digicon tube and scintillators, and 3) fabricating prototype Multi-Ray sensors for evaluation in the laboratory and under simulated reentry vibration environments. The results of Phase II proved that the Multi-Ray Ablation Sensor is an efficient miniature sensor assembly that is very attractive for use on high performance reentry vehicles. Vibration testing, however, showed that the sensor was effected by anticipated flight vibration levels (i.e., $0.8 \text{ g}^2/\text{Hz}$ at 45 grms). Phase III, funded under contract DNA001-76-C-0140, involved vibration hardening the sensor to vibration levels up to $0.8 \text{ g}^2/\text{Hz}$. The results of the vibration tests show that the sensor is essentially unaffected by vibration up to $0.4 \text{ g}^2/\text{Hz}$ with the entire sensor "hard" mounted. For the sensor to pass the $0.8 \text{ g}^2/\text{Hz}$ level, the sensor must use a vibration isolation system. With the sensor mounted on vibration isolators, the sensor performance was unaffected by vibration.

In the following sections, the sensor design and test data are presented. The design analyses, hardware fabrication and testing were conducted under contracts DNA001-75-C-0315 and DNA001-76-C-0140. Further sensor development tasks and environmental tests are being conducted under contracts DNA001-76-C-0310 and F04701-76-C-0041. The results of these tasks and tests will be reported at the completion of the respective contracts.

2.0 SENSOR DESCRIPTION

The Multi-Ray Ablation Sensor concept is illustrated in Figure 1. The sensor components are identified in the figure and include: 1) CsI scintillators, 2) fiber optic couplers, 3) nine-channel Digicon tube*, 4) high voltage power supply and filter, 5) preamplifiers, 6) amplifiers/discriminators, and 7) gas sealed structural container. A photograph showing the Digicon tube, fiber optics, scintillators, high voltage power supply, and hybridized amplifiers are shown in Figure 2. The gamma rays incident on the scintillators generate light (at ~ 0.4 microns) that travels along the optical fibers to the nine-channel Digicon tube. The Digicon tube converts the light into electrical pulses. The electrical pulses from the tube are input into low-noise, charge-sensitive preamplifiers and amplifier/discriminators to generate signals compatible with counters external to the hermetically sealed structure. The Digicon tube requires a -15 kV power supply and a high voltage filter to reduce ripple. To eliminate problems associated with high voltage, the high voltage supply/filter and Digicon tube are gas sealed.

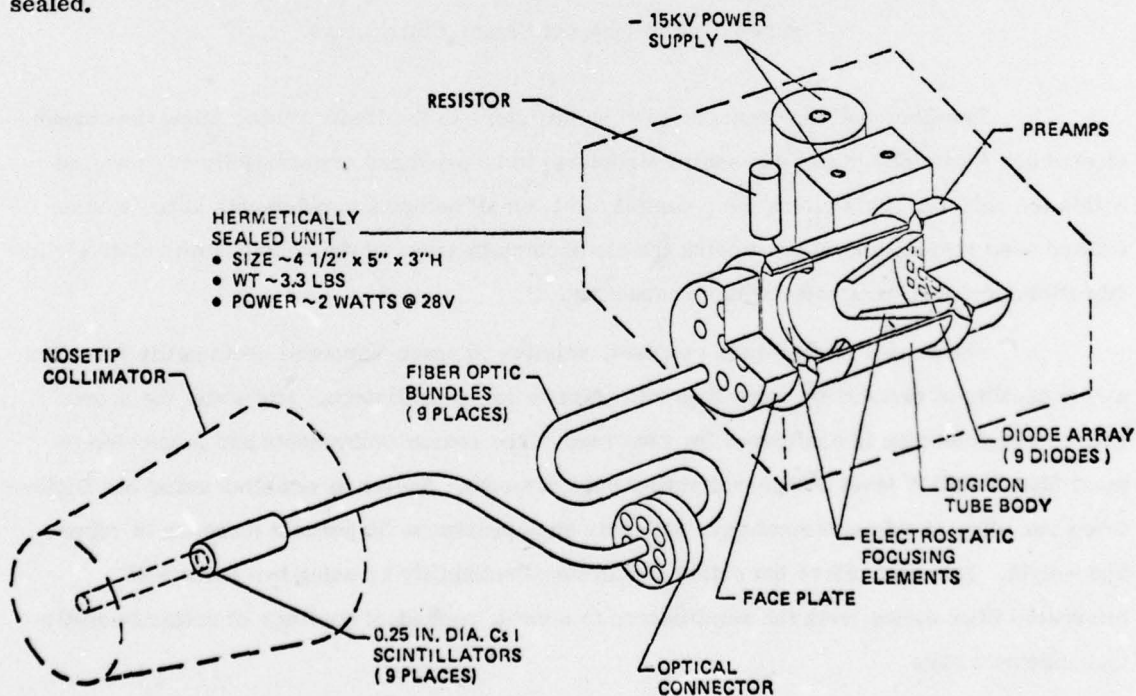


Figure 1. Nine-Channel Multi-Ray Sensor Schematic

* A class of digital photon-counting tubes manufactured by Electronic Vision, Co., a Division of Science Applications, Inc., La Jolla, California.

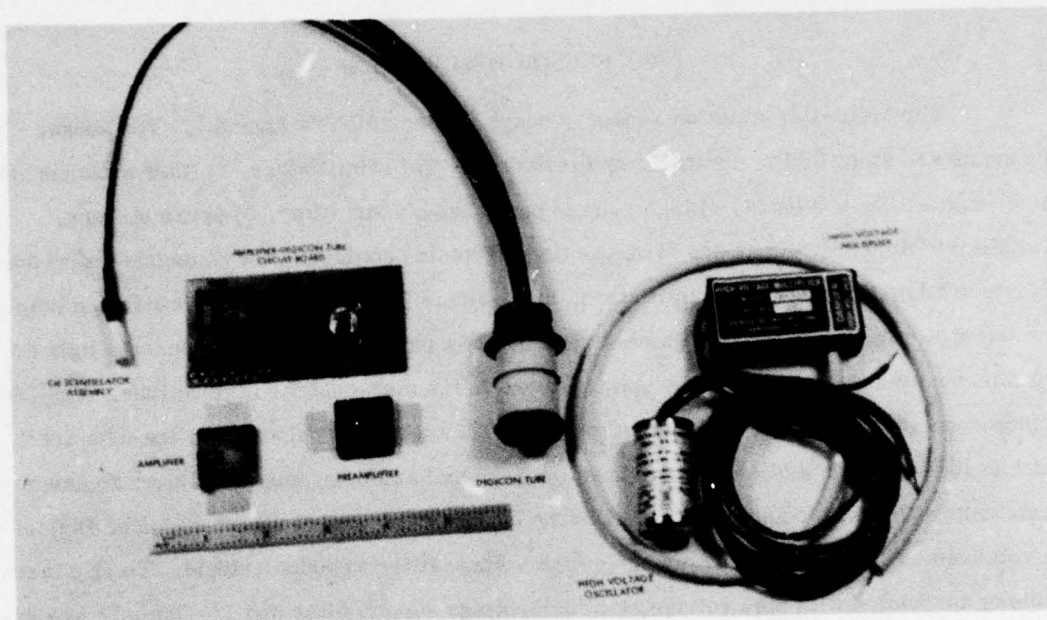


Figure 2. Nine-Channel Sensor Components.

The fiber optics, connecting the scintillators to the Digicon tube, allow the sensor electronics (contained in the gas-sealed structure) to be packaged at essentially any location within the vehicle. This offers the potential for 1) small detector subelements in the volume limited nose region, and 2) positioning the electronics in areas of the vehicle with relatively low vibration input and/or greater volume capability.

The sensor assembly is compact, relative to space-hardened photomultiplier tubes, and is capable of processing more than nine-gamma ray scintillators. Presently the sensor with one Digicon tube is configured for nine rays. The sensor components are fabricated to meet MIL-M-38510 level B high-reliability requirements. Sensor assemblies using two Digicon tubes can offer 18 measurement rays with only an approximate 30 percent increase in volume and weight. This also offers the option of increased reliability by using two tubes with bifurcated fiber optics from the scintillators to provide redundant readings of critical nosetip measurement rays.

Two nine-channel sensors, one with a discrete preamplifier and one with a hybridized preamplifier, have undergone functional vibration tests at 0.1, 0.2 and 0.4 g^2/Hz . For the sensor with a discrete preamplifier, no difference in static and dynamic count rates was found. For the sensor with a hybridized preamplifier, the static and dynamic count rate differed by less

than four percent. With the sensor vibration-isolated, no change occurred in the count rate at a vibration level of $0.8 \text{ g}^2/\text{Hz}$. A four-channel sensor, non-operating, has survived nine minutes of $0.4 \text{ g}^2/\text{Hz}$ vibration without any change in performance.

The nine-channel Digicon tube is illustrated schematically in Figure 3. When light from a scintillator impinges on the photocathode, photoelectrons are emitted and are accelerated up to energies of 15 kV. These energetic electrons are focused onto back-biased silicon diodes operated in the EBS (Electron Bombarded Silicon) mode. Focusing is accomplished by the electrostatic lens formed by the electrodes shown in the sketch. The photoelectrons are imaged one-to-one onto an array of nine silicon diodes (each 1 millimeter in diameter) with each diode viewing a particular area on the photocathode of about the same dimensions as the silicon diode. The tube gain is a function of the photoelectron voltage and the photoelectron energy (or threshold voltage) required to penetrate the "dead layer" on the diode's surface. Diode threshold voltages are typically 2 to 3 kV, and tube gains at 15 kV are between 3000 and 4000. The charge pulses from the silicon diodes are amplified by a set of low-noise electronics, the most critical component of which is an FET charge-sensitive preamplifier. Pulses exceeding a preset threshold are counted. The threshold is normally set between the electronic noise and the pulse height corresponding to a single photoelectron.

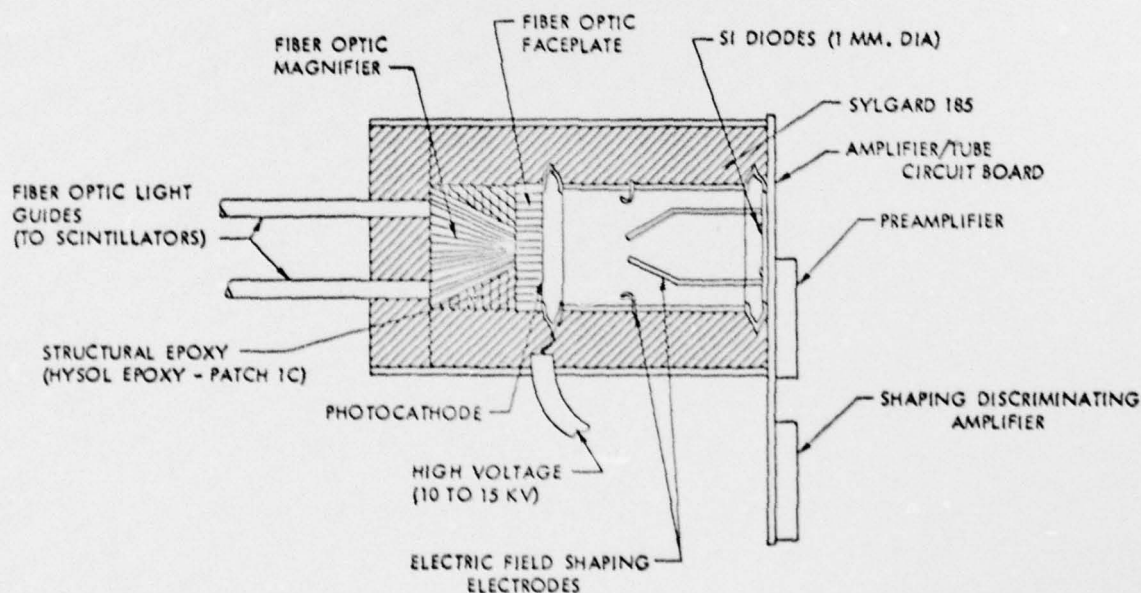


Figure 3. Schematic of 9-Channel Digicon and Amplifiers

3.0 SENSOR DESIGN

The sensor was designed to measure nosetip ablation (and heatshield ablation, if required) along nine rays. The sensor was configured to enable packaging the sensor electronics in essentially any location in the vehicle with only the scintillation detectors placed in the volume-limited nosetip region. The sensor signal-processing elements entail low-noise, charge-sensitive preamplifiers. The signal conditioning elements between the preamplifiers and vehicle telemetry have not been selected and are tasks for a future program. The objectives of the sensor design effort under Contracts DNA 001-75-C-0315 and DNA 001-76-C-0140 were to design, fabricate, and test a nine-ray sensor assembly that would convert incident gamma rays into corresponding electrical pulses. The pulses are to be processed with conventional signal conditioning hardware that has been used on other sensor systems.

The sensor design requirements and sensor electrical, mechanical, and optical design features are presented in the following subsections.

3.1 DESIGN REQUIREMENTS

The sensor design requirements were to: 1) configure the sensor for the Materials Screening Vehicle (MSV), and 2) design the sensor to operate in the environmental conditions typical of the Advanced Nosetip Test vehicle (A.N.T.) and the Technical Development Vehicle (TDV) flight test programs. In configuring the sensor for MSV, the design was to have minimal impact on the existing vehicle hardware with the design objective being a redesign of only the vehicle telemetry interface components.

The environmental conditions for which the sensor was to be designed have changed considerably during the program. The environmental conditions that were to be used in the design are presented in Table I. The various vibration test conditions that were imposed on the sensor throughout the sensor development program are presented in Figure 4. In contract DNA 001-75-C-0315, the $0.4 \text{ g}^2/\text{Hz}$ vibration test with a 2000 Hz maximum frequency was the baseline level. The goal in subsequent sensor development efforts, contracts DNA 001-76-C-0140 and F04701-76-C-0041, was the $0.8 \text{ g}^2/\text{Hz}$ vibration level of Figure 4.

3.2 ELECTRICAL DESIGN

An electronics block diagram for the Multi-Ray Ablation Sensor is shown in Figure 5. Photoelectrons emitted from the Digicon's photocathode are accelerated by the electrical field ($\sim 15 \text{ kV}$) between the photocathode and photodiodes. The photodiodes are placed on a header

Table 1. Sensor Environmental Design Requirements.

1. Temperature Cycle (Nonoperating). -35°F for 8 hours, increasing to 110°F within 5 minutes and maintain for 8 hours. Repeat 3 cycles.
2. Humidity (Nonoperating). MIL-STD 810B, Method 507 except maximum temperature = 110°F and 3 cycles.
3. Vibration (Operating). See Figure 4 for spectra, 40 seconds each axis.
4. Shock (Operating).

Frequency, HZ	Response, G's
20	35
33	60
58	100
76	260
90	260
220	170
400	700
5,800	2,900
10,000	2,900

Two Shocks Each Axis

5. Linear Acceleration (Operating).

Forward Longitudinal:	21 g	2 Minutes
Reverse Longitudinal:	190 g	1 Minute
Other Two Axes:	190 g	Both ways, 1 Minute
6. Acoustic Noise (Operating). MIL-STD-810B, Category D.
7. Temperature/Altitude (Operating). Stabilize at 110°F then reduce pressure to 0.17 mm Hg (or less) and hold for 30 minutes.

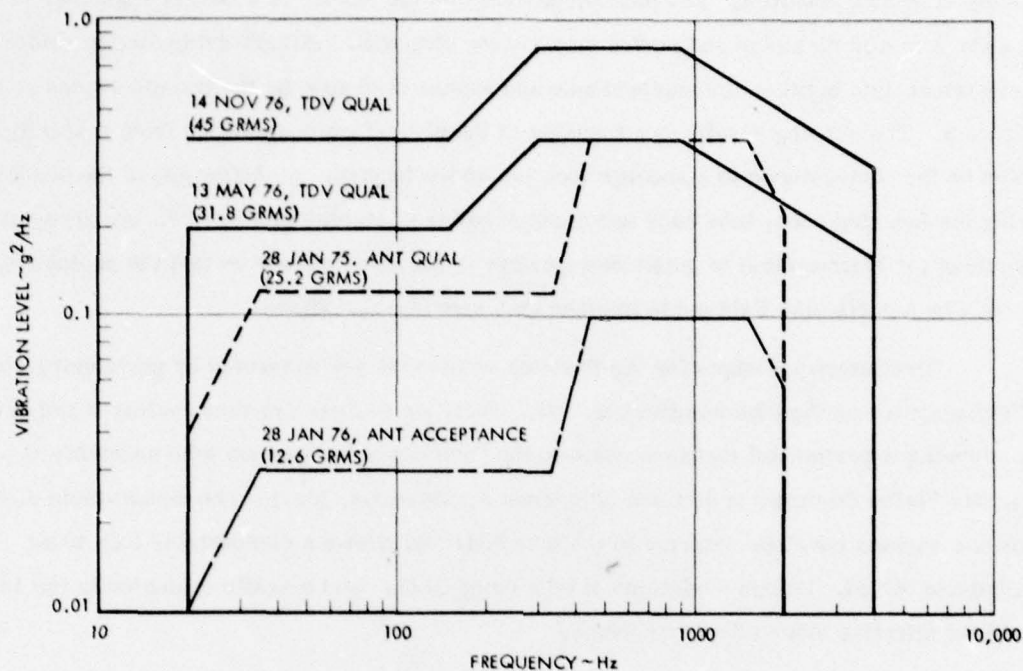


Figure 4. Multi-Ray Vibration Specifications.

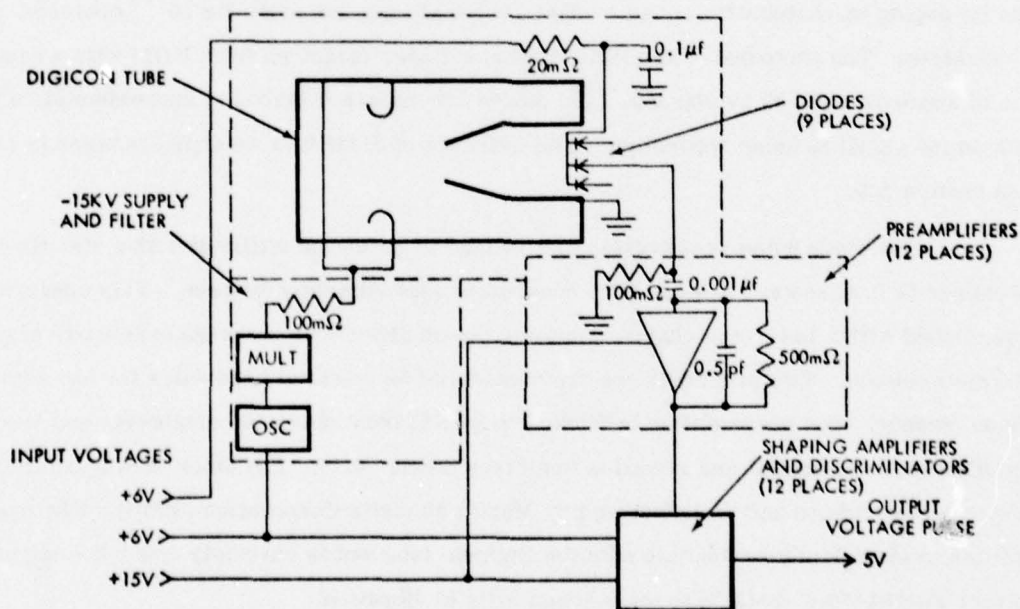


Figure 5. Multi-Ray Sensor Vehicle Electrical Schematic.

operating at ground potential. The photodiode array on the header is shown in Figure 6. The diodes are 1 mm in diameter and placed on a silicon chip with a silicon-gold eutectic solder. The electrical field between the photocathode and header is shaped by the two electrodes shown in Figure 3. The shaping results in a focusing of the photoelectrons emitted from a specific location on the photocathode to a specific location on the header. A photograph of the header showing the focusing cone, tube body and diode array is presented in Figure 7. An array of light guides (or fiber-optics) is positioned relative to the photocathode so that the photoelectrons generated by a particular light guide impinge on a specific photodiode.

Preliminary designs for the focusing electrodes are generated by performing electrical field analyses on the tube components. The electrode designs are then evaluated and refined by performing experimental measurements in the "demountable" vacuum tube assembly at Electronic Vision Company (a division of Science Applications, Inc.). The demountable assembly provides a vacuum envelope external to the tube body and allows a demountable tube to be installed and tested. Design variations of tube components can be easily evaluated in the assembly without affecting other tube components.

Detection of the photoelectrons from the photocathode are carried out in nine identical parallel signal channels. A schematic of one channel has been presented in Figure 5. Photoelectrons impinging on photodiodes cause a charge pulse of approximately 5×10^{-16} coulombs per photoelectron. The photodiodes are PIN040 silicon diodes (acquired from UDT) with a capacitance of approximately 25 picofarads. The diodes are reversed biased at approximately 6 volts to maximize signal to noise separation. The influence of diode bias on signal to noise is presented in Section 4.0.

The diode pulse is converted to a voltage of about one millivolt with a rise time of approximately $0.1 \mu\text{sec}$ and a decay time constant of approximately $30 \mu\text{sec}$. This conversion is accomplished with a low-noise charge-sensitive preamplifier with a charge sensitivity of two volts/picocoulomb. Two preamplifiers are considered as potential candidates for use with the Digicon sensor. One preamplifier is fabricated by SAI from discrete components and has successfully passed electrical and vibration tests (see Section 4.0). The other preamplifier is a six-channel hybridized unit manufactured by Martin Marietta Corporation (MMC). The preamplifier is electrically compatible with the Digicon tube and is currently under investigation in Contract F04701-76-C-0041 as to its susceptibility to vibration.

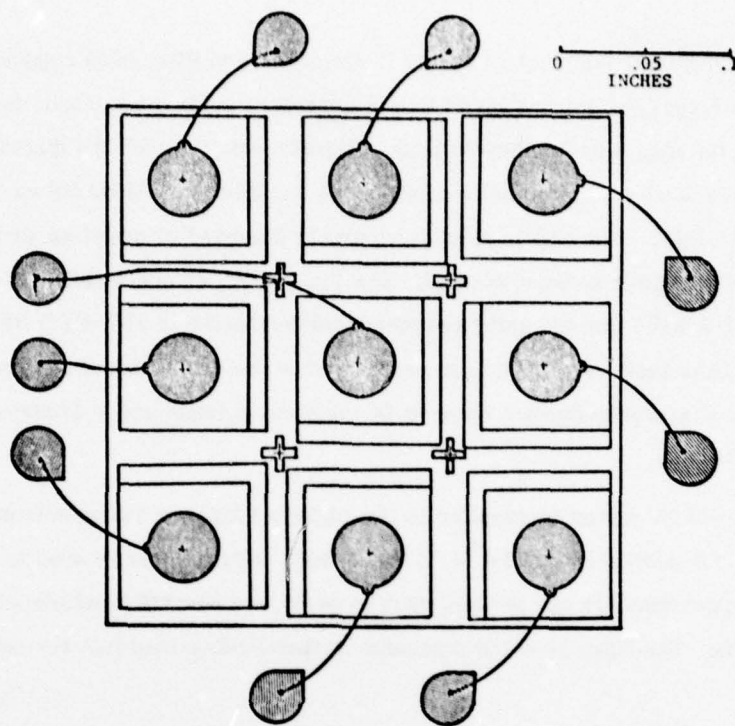


Figure 6. Header Design for Nine-Channel Digicon Tube

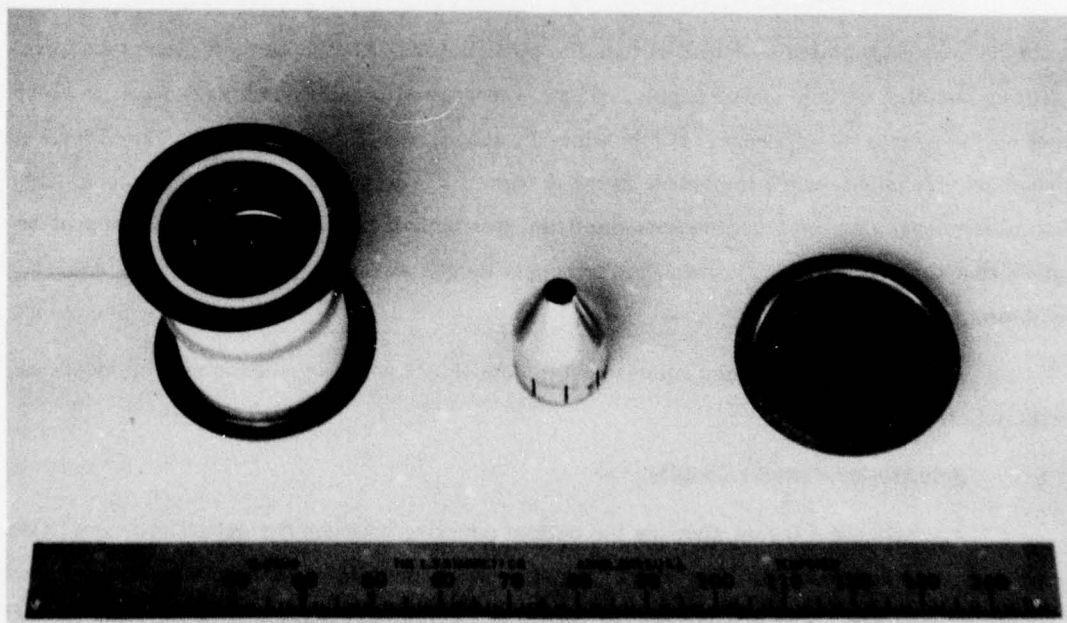


Figure 7. Nine-Channel Digicon Tube Components (Tube Body, Electrostatic Focus Cone, and Nine-Diode Array Header).

The preamplifier's output signal is amplified and filtered to reduce the signal bandwidth. The signal is then compared to a discrimination level set above the noise but considerably below the single photoelectron peak. Signals which exceed the discrimination level initiate 5 volt pulses which increment a counter. A candidate amplifier/filter/discriminator is manufactured by MMC. The unit is hybridized and is designed to interface with the hybrid preamplifier that is currently being evaluated. The preamplifiers and amplifiers meet the requirements of MIL-M-38510A and the units are inspected and tested to MIL-STD-883, level B. Only preliminary performance tests have been performed on the unit under the current program. Detailed electrical and environment tests on the unit are planned under Contract F04701-76-C-0041.

The -15 kV power is supplied to the Digicon tube by a Venus Scientific oscillator (Model 0-6.75) and multiplier (Model M-15N). A high voltage filter is used to reduce the power supply ripple (approximately one percent peak to peak) to a level compatible with the tube (less than 0.1 percent). The filter is a 100 megaohm resistor integrated into the sensor as shown in Figure 5.

3.3 MECHANICAL DESIGN

Mechanical design analyses have been performed on the sensor assembly. The components that were examined in detail include the scintillators, fiber optics, Digicon tube, preamplifiers and high voltage power supply. The environmental conditions that had the greatest impact on the sensor design were: 1) vibration, 2) shock, and 3) high altitude. The vibration and shock environments were important in the design of the scintillation crystal support, fiber optics attachment, Digicon tube, and preamplifier mechanical layout. High altitude operation required that the tube and high voltage power supply be gas sealed to prevent high voltage breakdown.

Discussions of the mechanical design details of the major sensor sub-elements are presented below.

3.3.1 Scintillator/Optical Coupling

A mechanical layout showing the optical coupling between the scintillator and Digicon tube is presented in Figure 8. The layout identifies the materials of each component in the optical coupling assembly. The critical stress region in the optical coupling is at the ends of the fiber optics. To provide efficient optical transmission, the fiber optics must be "butt-bonded" to the tube and scintillator with optical cement. Flexing of the multistrand fiber bundle can cause

high stresses on the butt bond because of differential movement of the individual fibers. The stresses induced by flexing, in addition to the fact that butt-bonds are inherently weak, makes the fiber ends a critical part of the design. To strain relieve the ends, a technique was developed that entailed epoxying the fibers and swagging a metal fitting over the fiber ends. In the strain relief operation, the following steps were followed:

1. A short section of the optical jacket is stripped off the fiber ends and the individual fibers are coated with clear epoxy (Hysol EK-20);
2. A metal fitting is inserted over the fiber end and is swagged over the cladded and uncladded fibers;
3. At the Digicon tube end, the fibers are attached to the tube with Hysol EK-20 using a butt joint;
4. After all fibers have been attached to the tube, the void around the fibers is filled with EA956 up to the edge of the metal fitting (see Figure 8). After curing of the EA956, the remaining void is filled with Sylgard 185;
5. At the scintillator end, the fiber is also coated with Hysol EK-20. The fiber is inserted into a lens-split collet fitting (supplied by Tap Plastics, Inc.), and the split collet nut is tightened to provide strain relief;
6. The lens fitting is bonded to a CsI crystal with Hysol EK-20;
7. The CsI crystal and lens are coated with TiO_2 epoxy paint;
8. The CsI-lens-fiber bundle is bonded into an aluminum tube with EA956 (Figure 8).

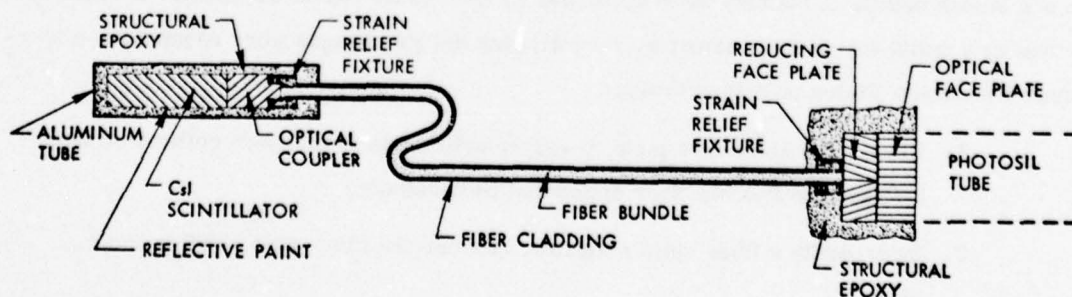


Figure 8. Scintillator and Optical Coupling.

These fabrication steps have resulted in optical assemblies that are rugged and have undergone severe flexing and vibration testing without any apparent change in performance. An aluminum tube is placed over the CsI crystal to provide structural support for the CsI/lens bond. The aluminum tube is bonded into a collimator with either EA956 or Sylgard 185, which represent 'hard' and 'soft' bonds, respectively. Both types of bonds have been evaluated under vibration with no apparent difference in performance.

CsI was selected as the scintillator material. CsI relative to NaI is less susceptible to shock and humidity. As described above, the scintillator is epoxied into an aluminum tube. This is a hard structural bond and provides structural reinforcement for the scintillator to fiber optic joints. Examination of a scintillator commercially mounted to withstand shock and vibration revealed that the scintillator was 'soft' bonded in an aluminum housing. The 'soft' bond, if required, can be placed between the aluminum housing and collimator.

Two basic types of fiber optics were evaluated for the scintillator to Digicon tube light coupling; plastic and glass. The glass fibers were found to be susceptible to breakage when subjected to flexing over small bend radii. The plastic fibers, on the other hand, were found to be extremely rugged with essentially the same optical transmissivity as the glass fibers. Plastic fiber fabricated by DuPont was selected for use on the sensor because of high transmission and good ruggedness. The fiber, Crofon 1610, has a core diameter of 0.088 inch and uses a 0.130 inch outside diameter jacket. The fiber diameter matches the effective area of the Digicon photodiodes after the diodes are magnified by the 2.8 magnifier (shown in Figure 3). The optical transmission measurements that were used to select the fiber are presented in Section 4.1.

3.3.2 Digicon Tube

A schematic of the Digicon tube has been presented in Figure 3. The basic fabrication and design details of the tube were developed by Electronic Vision Company. In order to use the tube as a multi-ray nuclear detector, the following design changes were required to a four-channel Electronic Vision phototube design:

1. Change the glass face plate to a fiber optic plate to maintain collimated light between the flexible fiber optics and photocathode;
2. Incorporate a fiber optic magnifier between the fiber optic bundles and face plate;

3. Increase the diode diameter (from 0.33 to 1.0 mm) to increase optical transmission from the 6.3 mm diameter scintillators;
4. Redesign the header to incorporate an array of nine 1.0 mm diodes;
5. Change the tube body from glass to ceramic (Al_2O_3) to aid in shock hardening.

These design changes did not represent major tube modifications. The critical tube processing steps that are required for the general class of Digicon tubes remain essentially unchanged for the multi-ray detector. The steps required to manufacture a tube photocathode surface without destroying the silicon diodes involve forming the alkali photocathode on the faceplate and transferring the unit to the tube body where they are attached by copper cold welding. These procedures are designed to avoid "poisoning" of the silicon diodes during photocathode manufacture and prevent photocathode deterioration which occurs at temperatures above $\sim 50^\circ\text{C}$.

The fiber optic faceplate provides a vacuum envelope and prevents divergence of the light between the fiber optic bundles and photocathode. In order to control the image size on the photocathode, the light exiting the fiber optics must remain collimated through the vacuum seal. With the fiber bundles coupled to glass, the light divergence half angle is approximately 46° . Using a glass faceplate for the vacuum seal will cause considerable light divergence and an unacceptable photocathode image diameter (an image diameter of approximately 0.15 inch). The use of a fiber optic faceplate will maintain a collimated light source and an image diameter that is comparable to the diode diameter of 0.040 inches.

The incorporation of a fiber optic magnifier between the fiber bundles and a faceplate is to facilitate installation of the fiber bundles onto the Digicon tube. The magnifier is used to magnify the diode array at the plane where the fiber bundles are to be attached. This results in increased spacing between the fibers and allows volume for the metal fitting required at the fiber ends.

The diode diameter was increased from 0.33 to 1.0 mm. This change was implemented in order to minimize the reduction in optical transmission that is introduced by the change in diameter between the scintillator (6.3 mm diameter) and the diode image on the photocathode. The reduction in optical transmission is a function of the ratio between diode image area and scintillator cross-sectional area. Increasing the diode diameter to 1.0 mm improves the optical efficiency by a factor of approximately 9.

A redesign of an existing four-channel header was required to incorporate an array of nine-1.0 mm diodes. The redesign required laying out the diodes within the electrostatic focusing area of the tube with sufficient spatial separation to essentially eliminate electrical crosstalk. A square array, shown in Figure 6, was selected for the nine-channel tube with 2.7 mm between diode centers. As will be shown in Section 4.0, the electrical crosstalk between adjacent diodes is less than 0.5 percent of the diode signal.

The tube body was changed from glass to alumina to increase the structural hardness of the tube. Relative to glass, an alumina tube offers increased tube body strength and increased hardness at the tube to metal joints. With alumina, the metal seals are brazed to the ends of the tube; whereas with glass, metal to glass fuzing is required that inherently induces relatively high residual stresses in the components.

3.3.3 Preamplifiers

A number of low-noise, change-sensitive preamplifiers were investigated in order to identify candidate preamplifiers most suitable for amplifying the Digicon tube output signals. Important criteria for selecting a preamplifier were as follows:

1. Adequate low-noise performance which will permit good separation of the single photoelectron peak from the noise in the Digicon tube pulse-height distribution,
2. Minimum vibration sensitivity,
3. Compact size, since nine preamplifiers are to be packaged with each Digicon tube.

For laboratory testing of prototype tubes, a commercially available discrete component preamplifier manufactured by Nuclear Equipment Corporation was used.* The electrical performance of this preamplifier was excellent, as will be shown in Section 4.0 by the tube pulse height distribution. The NEC preamplifier, while demonstrating excellent performance in the laboratory, is unsuitable for use in the multi-ray sensor because of its large size and extreme microphonic sensitivity.

* Nuclear Equipment Corporation Model 336

Table 2 summarizes the results of a preliminary investigation that was aimed at identifying an optimum preamplifier for use in the sensor. Three hybrid designs (Rockwell International, Philco-Ford, and General Electric) could be eliminated because of inadequate low-noise performance with the Digicon tube. The two most promising candidates are the Martin six-channel hybrid and the SAI discrete preamplifiers. The Martin hybridized preamplifier is very attractive since it is completely developed and is quite compact (the six-channel preamplifier is contained in a "flat pack" about 2.5 cm x 2.5 cm x 0.5 cm thick). The SAI discrete component design can be packaged to meet sensor volume constraints; however, the amount of space devoted to preamplifiers would have to be significantly greater than for the hybrid design.

Table 2. Summary of Preamplifier Development Effort.

PREAMP DESIGNATION	CONSTRUCTION	ELECTRICAL TESTS	VIBRATION TESTS	STATUS (1/76)
MARTIN DENVER	HYBRID (6-CHANNEL)	MARGINAL, POSSIBLE IMPROVEMENT WITH SELECTED FET	--	FET TO BE SELECTED VIBRATION TESTS RECOMMENDED IF ELECTRICAL PERFORMANCE ACCEPTABLE
MARTIN DENVER NOAA	HYBRID (1-CHANNEL)	GOOD	FAILED VIBRATION	MOUNTING AND POTTING INVESTIGATION RECOMMENDED AS BACKUP FOR 6-CHANNEL UNIT
SAI	DISCRETE BREADBOARD	GOOD, POSSIBLE IMPROVEMENT WITH SELECTED FET	SLIGHTLY MICROPHONIC	CONSIDERABLE IMPROVEMENT ACHIEVED FURTHER HARDENING RECOMMENDED
NEC	DISCRETE	EXCELLENT	VERY MICROPHONIC	UNSUITABLE FOR FLIGHT
PERKIN-ELMER	DISCRETE BREADBOARD	GOOD	--	POSSIBLE BACKUP DESIGN
ROCKWELL INTERNATIONAL	HYBRID (4-ELEMENT)	EXCESSIVE NOISE	--	UNSUITABLE
PHILCO-FORD	HYBRID (2-ELEMENT)	EXCESSIVE NOISE	NOT MICROPHONIC	CANNOT BE USED WITHOUT COMPLETE REDESIGN
GENERAL ELECTRIC	HYBRID	EXCESSIVE NOISE	--	UNSUITABLE

The SAI and Martin preamplifiers take an input pulse of approximately 3000 electrons and amplify the pulse to about 1 millivolt. Because of the relatively small input pulse, the connection between the diode and preamplifier can induce electrical noise by capacitance pick-up during vibration. A variation in capacitance between the connection and adjacent wires or a

ground plane caused by lead wire movement will introduce noise. To minimize lead wire movement, it was necessary to mount the preamplifier on the backface of the Digicon tube diode header. The preamps are mounted on a circuit board and the circuit board is in turn bonded onto the diode header as shown in Figure 3. Connections between the diode and preamplifier are made with posts mounted in the tube header. This design mechanically attaches the preamplifier to the diode header and connections are made with short, stiff posts.

3.3.4 High Voltage Supply and Gas Seal

The Digicon tube operates on -15 kV. The power is supplied by a Venas Scientific oscillator (Model 0-6.75) and multiplier (Model M-15N). The supply weighs a total of 8.5 ounces and can be packaged in less than 6 in³. A high voltage filter is used to reduce the output ripple of the multiplier. The filter is a 100 megaohm resistor (0.3 inch in diameter x 1.0 inch long).

To prevent high voltage breakdown during high altitude operation, all high voltage components are packaged in a gas sealed container. The components in the container include the Digicon tube, preamplifiers, high voltage oscillator/multiplier, and a high voltage filter. The gas sealed envelope also serves as the structural mount for the internal components and connectors. A preliminary design of the envelope for MSV is presented in Figure 9. The fiber optic bundles coupling the scintillators and tube penetrate the sealed envelope via a fiber optic seal. The fiber optic seal design is presented in Figure 10. Strain relief of the fiber optics is required between the tube and optic seal to relieve axial strain induced by vibration. Strain relief is achieved by: 1) putting a bend in the fiber between the tube and optic seal (Figure 9), and 2) 'soft'-mounting the fibers in the optic seal with a silicon rubber.

To minimize electromagnetic and/or RF interference, the Digicon tube is encapsulated in an aluminum case with Mu-metal. The sealed structure is aluminum with Mu-metal placed on the inside surfaces. The tube case is bolted to the sealed structure. The high voltage supply and filter will either be potted in place or encapsulated in a metal case and bolted to the structure. The method of attaching high voltage components will depend upon the available volume.

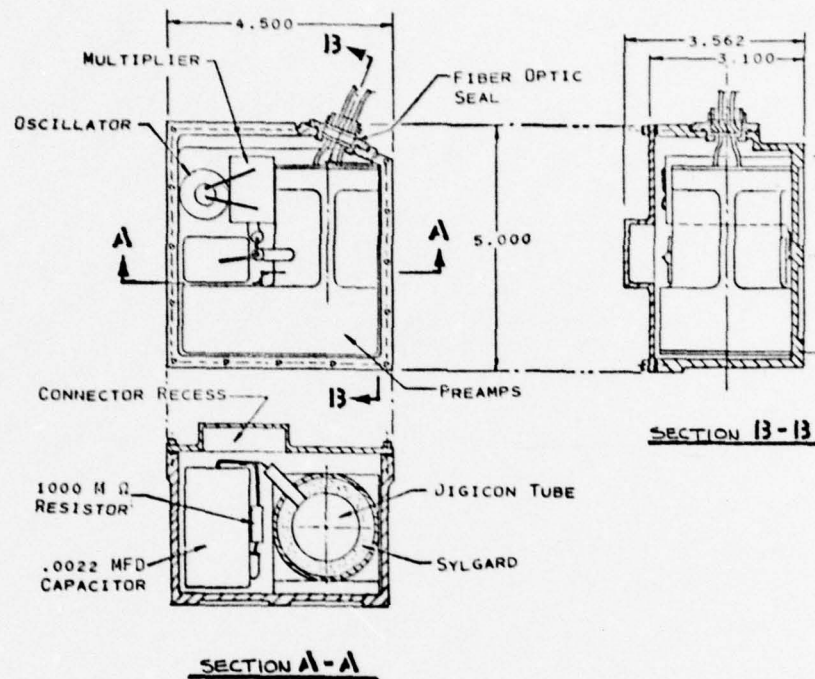


Figure 9. Multi-Ray Detector Container

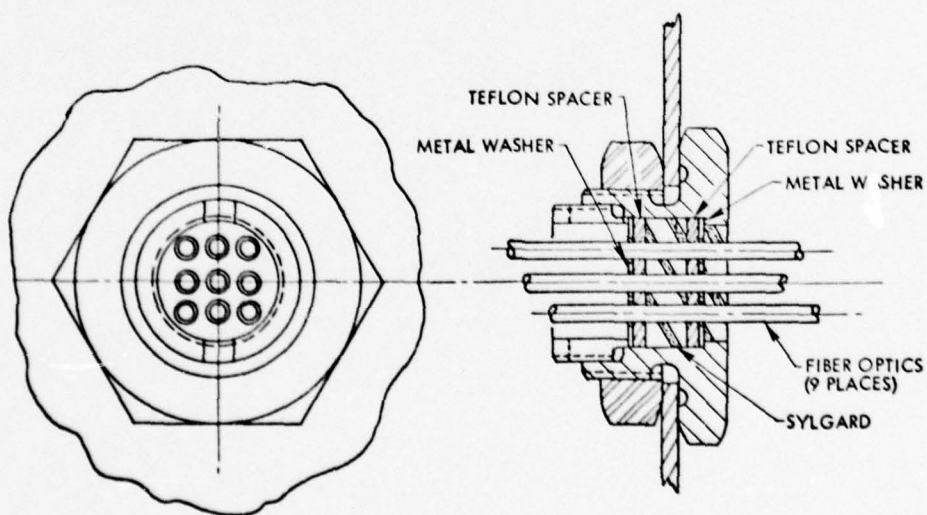


Figure 10. Fiber Optic Seal

4.0 SENSOR PERFORMANCE

Performance measurements have been made on three Digicon tubes and with two of the tubes in flight prototype sensor configurations. Electrical and optical measurements performed on the tubes show excellent reproducibility of performance between tubes, good signal-to-noise separation, and excellent focusing properties. Electrical and nuclear measurements performed on the flight prototype assemblies show high gamma-ray detection efficiency and sufficient electrical response to measure the counting rates needed for flight test (10,000 to 20,000 cps). Functional vibration tests have been performed on all three Digicon tubes. Vibration tests on the tubes at $0.4 \text{ g}^2/\text{Hz}$ produced no measurable change in count rate with a discrete preamplifier and less than a four percent change in count rate with a hybridized preamplifier. Vibration isolation of the tube and hybride preamplifier resulted in no measurable change in count rate at $0.8 \text{ g}^2/\text{Hz}$ vibration levels.

The optical, electrical, and nuclear performance measurements are summarized in the following paragraphs. The performance measurements and vibration test data that were generated under Contracts DNA001-75-C-0315 and DNA001-76-C-0140 are presented in detail. Efforts are currently in progress under Contracts DNA001-76-C-0310 and F04701-76-C-0041 to improve the sensor's performance under vibration. These efforts will be reported at a later date under the respective contracts.

4.1 OPTICAL PERFORMANCE

Optical transmission measurements were made to support the design and selection of the optical system that couples the scintillators to the Digicon tube. A schematic of the optical system has been presented in Figure 8. The transmission measurements were made with an SAI Photometer, a CsI scintillator, and a ^{137}Cs radioactive source in the configurations presented in Figure 11. The scintillator was painted with TiO_2 reflective paint on all surfaces except for the face where the optical coupling is attached. The baseline case to which all transmission measurements are referenced is noted in the figure and corresponds to the situation wherein the scintillator is bonded directly to an equal diameter photocathode.

In the transmission measurements, two components in the optical system were studied in detail; the scintillator to fiber optic attachment and the fiber optic cable. The attachment studies are summarized in Figure 11. A simple 'butt' joint was found to be superior to a spherical lens. The spherical lens data presented in the figure were for the optimum spacing between the scintillator and lens. The butt joint measurements indicate that, relative to the baseline case, the

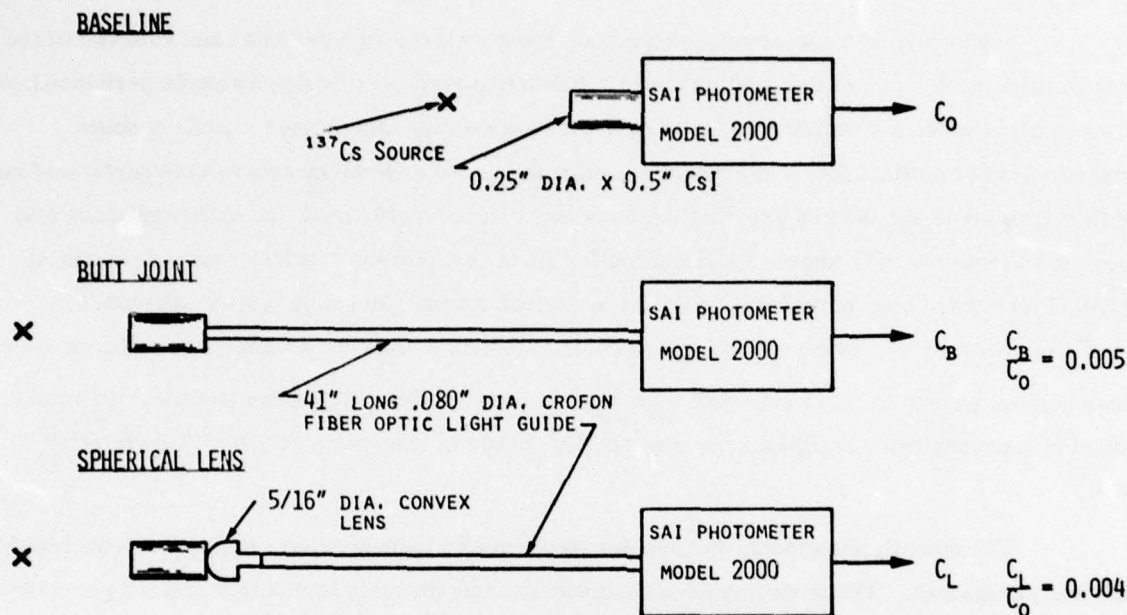


Figure 11. Transmission Measurements For Fiber Optic Light Guide.

transmission efficiency is 0.5 percent. This compares within a factor of two of the 1.0 percent efficiency computed using vendor supplied data and scaling the loss in transmission at the scintillator attachment by the reduction in area ratio. The optical fiber is 0.088 inches in diameter and approximately 80 percent of the area is light guide. The reported vendor transmissivity for the light guide at 0.4 microns (light output of CsI is around 0.39 to 0.42 micron) is 0.20 with an estimated 0.80 reduction in transmission at each end. With these data and a 0.25-inch diameter scintillator, the expected efficiency is 1.0 percent. The difference between the measured and computed efficiency could be attributed to scintillator end losses because the aft end of the scintillator was not painted with reflective paint. This could cause some light to be lost through the annulus between the fiber diameter and scintillator diameter.

The fiber optic transmission measurements were made using the 'butt' joint configuration of Figure 11. The results of the investigation of the fiber optic cables and the transmission measurements are summarized in Table 3.

Table 3. Fiber Optic Cable Transmission Measurements.

CABLE TYPE	BUNDLE DIAMETER (Inches)	LENGTH (Inches)	RELATIVE TRANSMISSIVITY
1610 Crofon, Pastic	0.088	24	1.0
1056 Crofon, Plastic	0.056	24	0.65
PFX Dupont, Plastic	0.046	24	0.10
5012 Corning, Glass	0.078	24	0.55

Of the fibers tested, the 1610 Crofon had the highest transmission. This fiber has 64-0.010-inch diameter individual fibers. The 1056 Crofon has a single fiber with a transmissivity that is 65 percent of the 1610 Crofon. The 5012 glass fiber offers good mechanical flexibility, but has low optic transmission. The vendor reported transmission versus fiber length is presented in Figure 12.

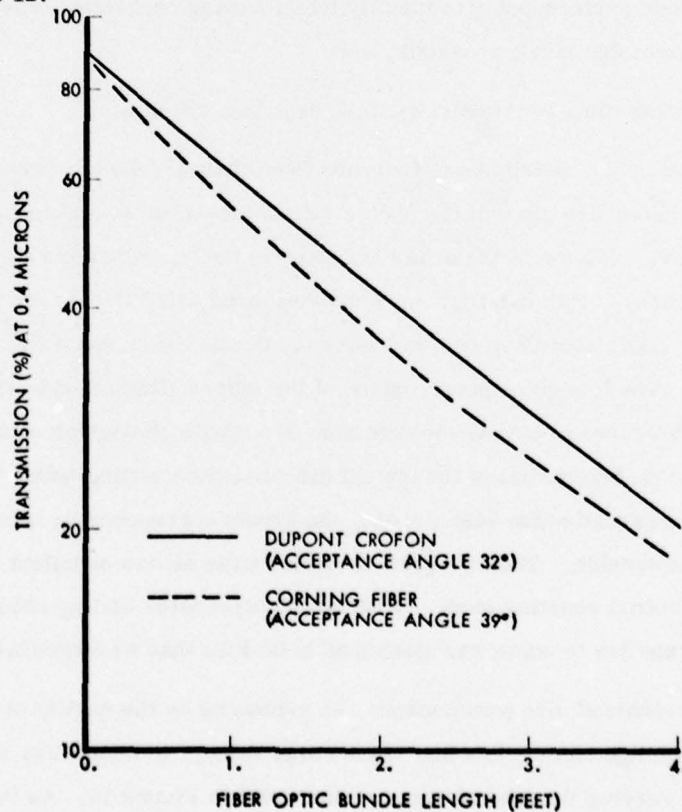


Figure 12. Transmissivity of Candidate Fiber Optics.

The optical coupling studies show that a significant amount of the light is lost in the reduction from the scintillator to fiber optics. The studies of Reference 2 show that a conical reducer offers no significant advantage over a fiber to scintillator butt joint. In Reference 3 an investigation was made to identify the optimum optical reducer for scintillators. The optimum reducer was concluded to be a parabolic configuration and offers, relative to a conical reducer, less than a factor of two improvement in transmission. For an overall optical system efficiency of 0.5 percent, a factor of two improvement is relatively insignificant. Because of the relatively small improvement, the parabolic configuration was not investigated further.

4.2 ELECTRICAL PERFORMANCE

Electrical performance tests have been performed on three prototype sensor assemblies. The tests have entailed the following measurements:

1. Pulse height distributions of Digicon tube/preamplifier output to identify signal to noise separation,
2. Cathode surface scans to identify tube focusing characteristics and tube-related (electrical) crosstalk, and
3. Counting rates to measure nuclear detection efficiency.

The pulse height distributions from the four-channel tube are presented in Figures 13 and 14. The distributions are plots of the photon counts measured at specific photon energy deposition levels (keV). Figure 13 identifies the electric noise, signal and the optimum region for discriminator setting. The distributions were measured using the sensor assembly of Figure 2, a Nuclear Equipment Corporation Model 336 preamplifier and a CO^{60} source to irradiate the CsI scintillator. The low-noise performance of the tube is illustrated by the excellent separation between the peak corresponding to the detection of a single photoelectron and the tube noise (sharp increase at pulse heights below the typical discriminator setting noted in Figure 13). In Figure 14, with the expanded pulse height scale, the events corresponding to multiple photoelectrons are clearly discernable. The high peak-to-valley ratio allows excellent gain stability even in the single photoelectron counting mode. With the discriminator setting shown in Figure 13, the measured counting rate due to noise was measured to be less than 10 counts/sec.

The four-channel tube performance, as evidenced by the quality of the pulse height distribution, was investigated as a function of tube high voltage and amplifier shaping time constant. The effect of varying the tube voltage is illustrated in Figure 15. As the voltage is

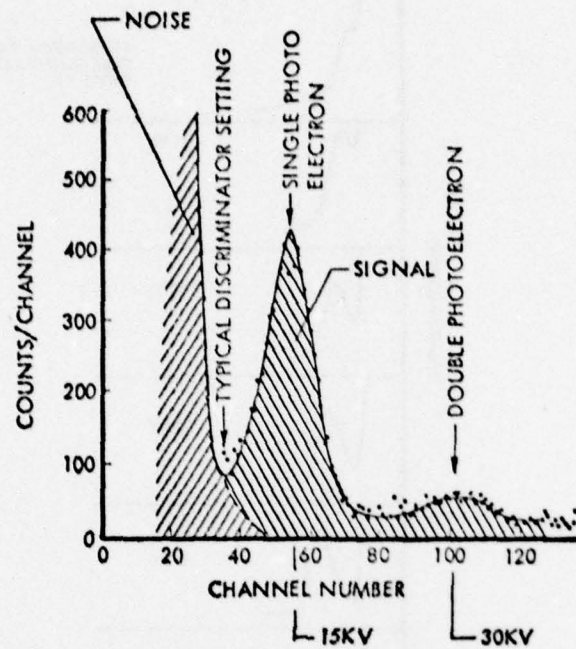


Figure 13. Typical Pulse Height Distribution from the Digicon

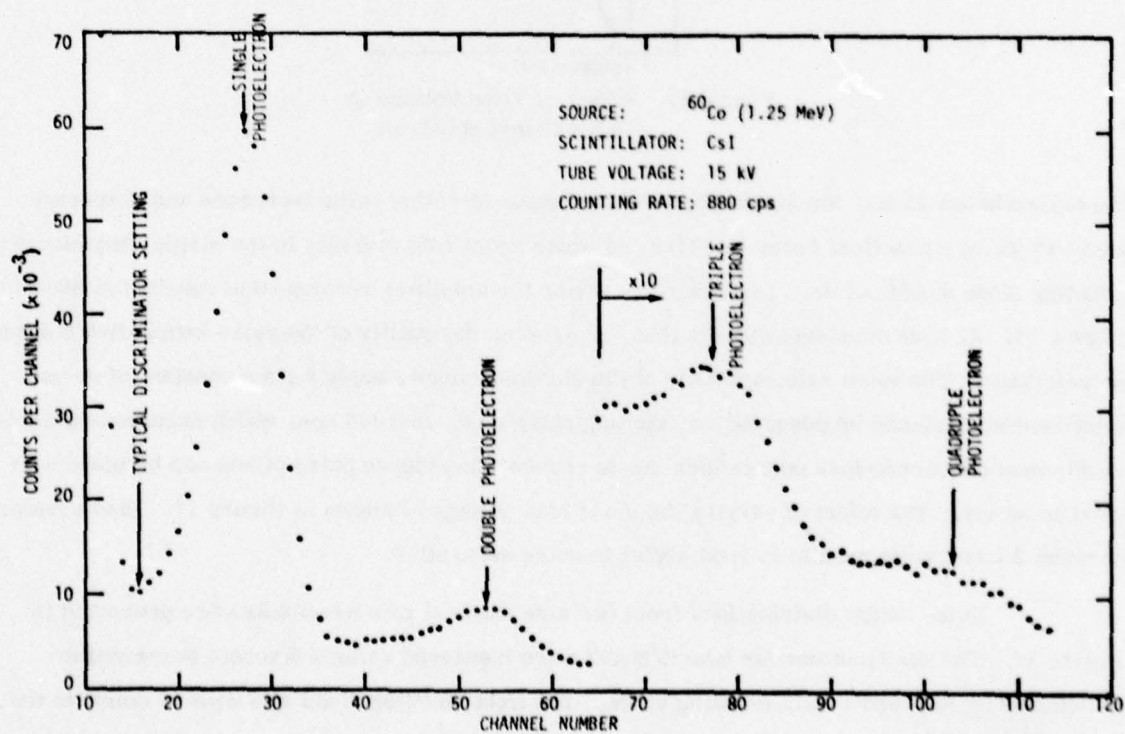


Figure 14. Four-Channel Digicon Tube Pulse Height Distribution

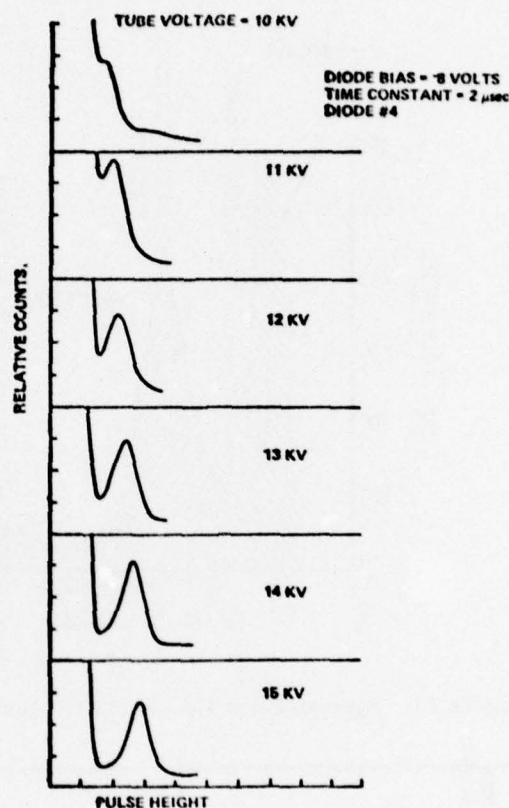


Figure 15. Effect of Tube Voltage on Pulse Height Spectrum.

decreased below 15 kV, the single photoelectron peak-to-valley ratio decreases and it appears that ~13 kV is a practical lower limit beyond which count rate stability in the single photoelectron counting mode would suffer. The effect of varying the amplifier shaping time constant is shown in Figure 16. At time constants shorter than $\sim 1.0 \mu\text{sec}$, the quality of the pulse height distribution deteriorates. The count rate capability of the ablation sensor, using a time constant of several microseconds, should be adequate for counting rates up to $\sim 50,000$ cps, which exceeds anticipated requirements. Count-loss corrections due to chance-coincidence pulse pileup can be made with good accuracy. The effect of varying the diode bias voltage is shown in Figure 17. Bias voltages between 2 and 8 volts results in good signal to noise separation.

Pulse height distributions from two nine-channel tube assemblies are presented in Figure 18. The distributions for tube S/N 352 were measured using a discrete preamplifier (fabricated by SAI) and a light emitting diode. The light emitting diode was used to simulate the light pulses generated by a CsI scintillator. Actual scintillators/radioactive sources could not be used because vibration test schedules for the assembly did not allow time to attach scintillators

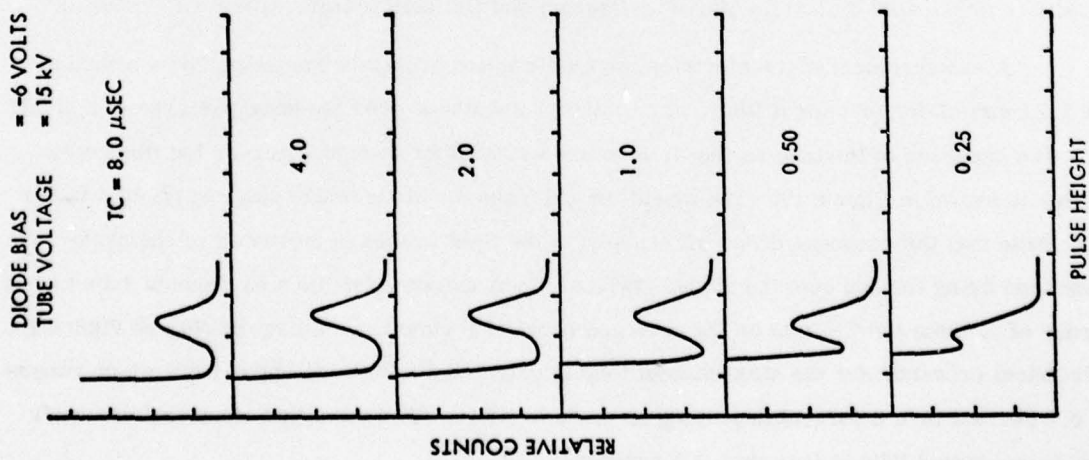


Figure 16. Effect of Amplifier Shaping Time Constant on Pulse Height.

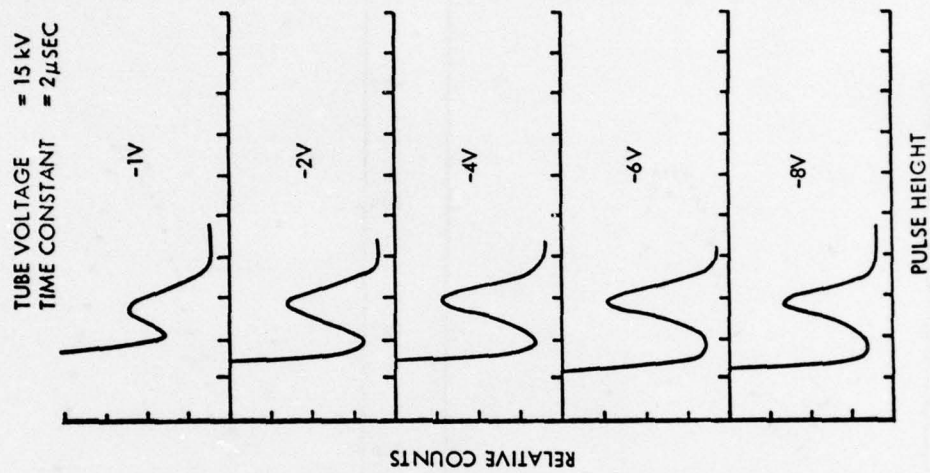


Figure 17. Effect of Diode Bias Voltage on Pulse Height.

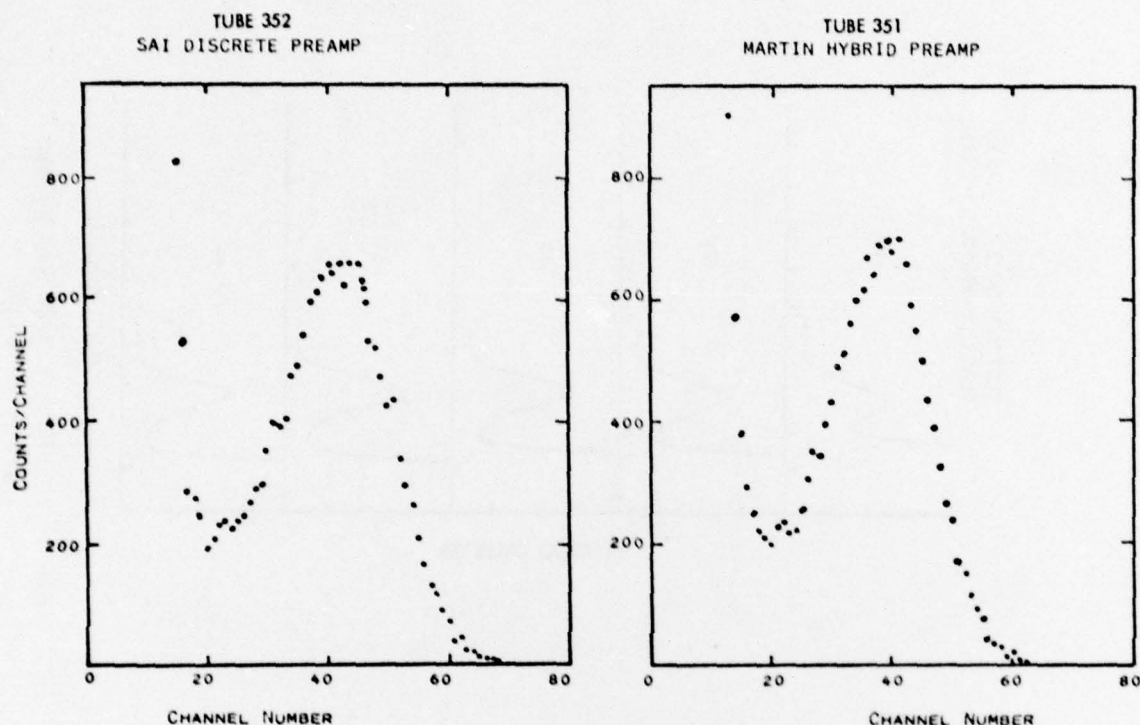


Figure 18. Nine-Channel Digicon Pulse Height Distributions.

and fiber optics. The distributions for tube S/N 351 were measured using a hybridized preamplifier (fabricated by Martin Marietta-Denver) and CsI scintillators with a ^{60}Co source.

A measurement of the electrical or tube-related crosstalk was obtained by scanning with a 2.24 mm diameter optical fiber, across the photocathode over the sensitive area of a single diode. The response of the tube as the illuminated optical fiber is moved across the fiber optic magnifier is shown in Figure 19. The magnifier enlarges the diode image plane by about a factor of 2.8. Note that the response drops off sharply as the light source is moved off of the photocathode area being imaged onto the diode. Typical diode spacings for the nine-channel tube are on the order of 2.7 mm (or 7.6 mm on the enlarged scale of Figure 19). Using the data of Figure 19, the electrical crosstalk for the nine-channel tube is calculated to have an upper limit which ranges from 0.8 percent to 1.8 percent depending on diode location. The measured electrical crosstalk for the four-channel tube is less than 0.5 percent.

Figure 20 presents the measured detection efficiencies of the four-channel tube with 0.25 inch x 0.5 inch and 0.25 inch x 1.50 inch CsI scintillators. In both cases the scintillators were coupled to the tube by a 24-inch long optical fiber (0.089 inch diameter). It may be noted

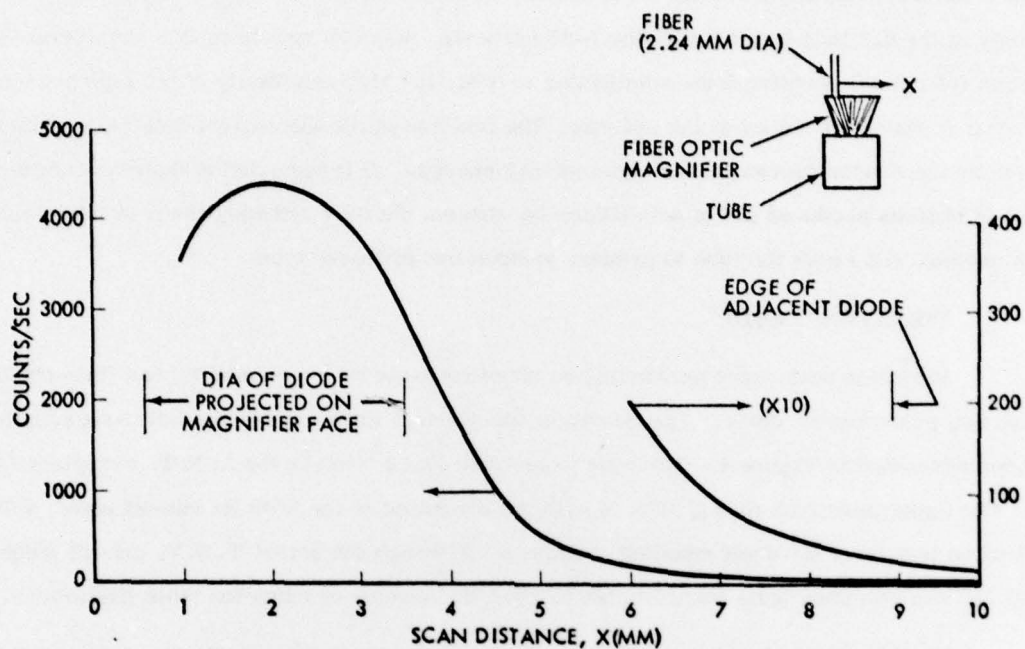


Figure 19. Response of Digicon Tube to Scan Across Fiber Optic Magnifier.

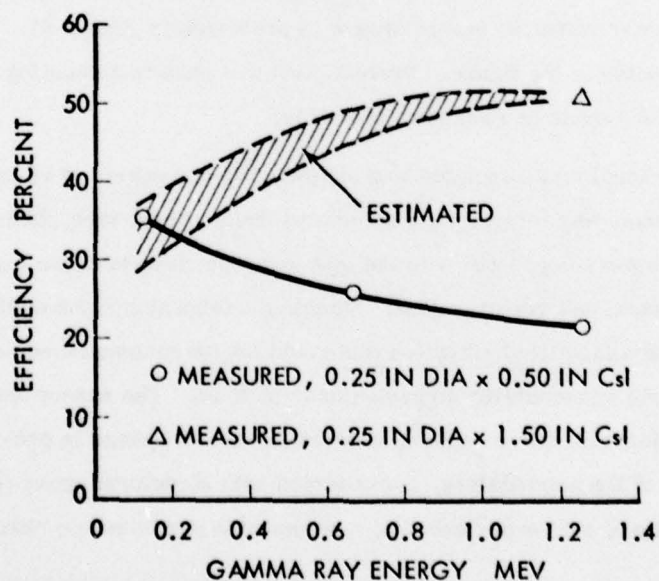


Figure 20. Measured Nuclear Efficiencies of Sensor.

that the measured counting efficiency at 1.25 MeV is very close to the theoretical detection efficiency of the 0.5 inch long scintillator (~25 percent). Even though there is a considerable loss of light in the optical coupling from scintillator to tube, the high sensitivity of the tube preserves the overall counting efficiency of the system. The fraction of the theoretical detection efficiency achieved by the sensor decreases with gamma-ray energy. It is expected to decrease because the number of photons produced in the scintillator decreases, thereby reducing the probability that enough photons will reach the tube to produce at least one photoelectron.

4.3 VIBRATION TESTS

Vibration tests were performed on three separate tube assemblies; one four-channel tube and two nine-channel tubes. The vibration spectra that were used in the tube assembly tests have been presented in Figure 4. The lower spectrum ($0.1 \text{ g}^2/\text{Hz}$) is the A. N. T. acceptance test level. The upper spectrum ($0.4 \text{ g}^2/\text{Hz}$) is with the exception of the 2000 Hz cut-off level, a T. D. V. qualification test level for shelf mounted hardware. Although the actual T. D. V. cut-off frequency is 4000 Hz, the vibration tests were limited to 2000 Hz because of vibration table limitations.

The hardware tested in each of the three series of vibration tests are summarized in Table 4. The test procedures and electrical support equipment are presented in Reference 4. Basically, all tube and scintillator related hardware were subjected to the vibration environments and all signal and power conditioning electronics were mounted off the vibration table. An electrical schematic of the sensor vibration test hardware is presented in Figure 21. The hardware subjected to vibration are noted in the figure. Pretest, test and post-test counting rates and pulse height measurements were made on each tube assembly.

The four-channel tube assembly was subjected to two series of vibration tests. The objective of the first series was to verify the structural design of the tube, fiber optics and scintillators. The tests were conducted with the tube non-operating because a preamplifier was not available to support a functional vibration test. Mounting a laboratory preamplifier off the vibration table and conducting a functional vibration test could not be accomplished because of the low diode output signal and its susceptibility to capacitance pick-up. The sensor was subjected to nine minutes of $0.4 \text{ g}^2/\text{Hz}$ vibration (three minutes each axis) with no change in pre- and post-test performance. Also, none of the scintillators, one mounted with structural epoxy (EA 956) and the other soft-mounted (Sylgard 185) experienced any measurable performance change.

The second series of vibration tests on the four-channel tube was conducted with a Martin NOAA hybrid preamplifier. The preamplifier was borrowed from Martin to support the

Table 4. Sensor Hardware Subjected to Random Vibration Tests.

DIGICON TUBE	HARDWARE VIBRATION TESTED	MAXIMUM VIBRATION LEVEL
4-channel	<ul style="list-style-type: none"> • Digicon Tube • Fiber Optics • Scintillators • Optical Seal • Hybrid Preamp (1-channel) • High Voltage Filter 	$0.4 \text{ g}^2/\text{Hz}$
9-channel (S/N 352)	<ul style="list-style-type: none"> • Digicon Tube • Discrete Preamp (2-channel) • High Voltage Filter 	$0.4 \text{ g}^2/\text{Hz}$
9-channel (S/N 351)	<ul style="list-style-type: none"> • Digicon Tube • Fiber Optics • Scintillators • Hybrid Preamp (6-channel) • High Voltage Filter 	$0.8 \text{ g}^2/\text{Hz}$

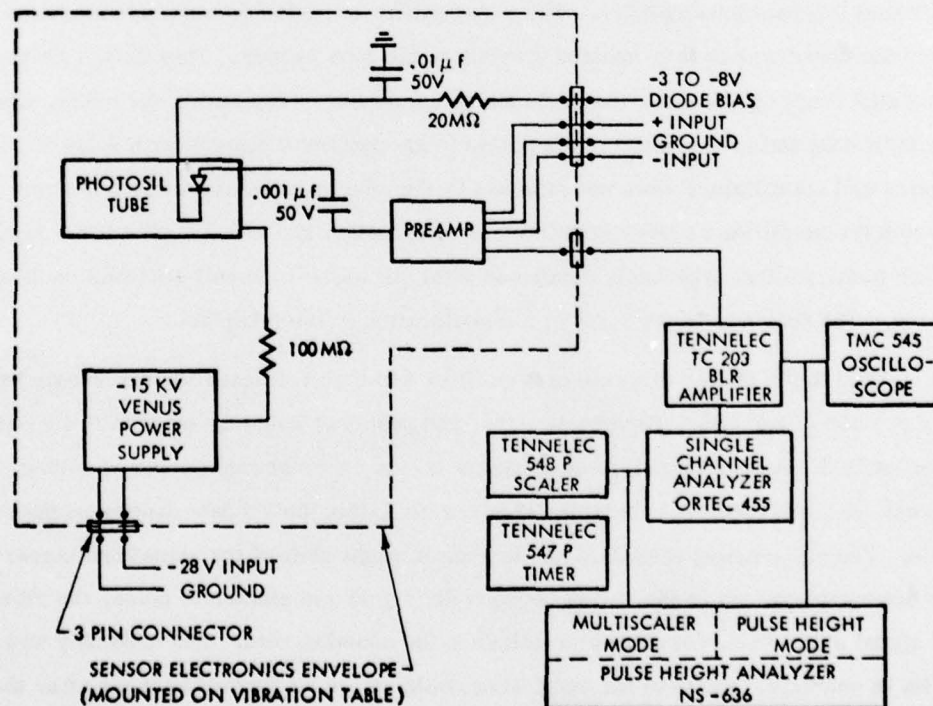


Figure 21. Typical Sensor Vibration Test Electrical Schematic.

test because the Martin six-channel hybrid preamplifier (to be used with the Digicon tube) was in development. Since the preamplifier was borrowed, a temporary mount was constructed in which the preamplifier was spring-loaded and approximately one-inch leads were required to connect the tube diodes and preamplifier. This type of mounting proved to be totally inadequate. At vibration levels of $0.1 \text{ g}^2/\text{Hz}$, the tube/preamplifier assembly exhibited excessively high vibration-induced noise. In order to establish the noise as being tube or preamplifier-related, all power leads to the tube were disconnected and the preamplifier output was monitored. The preamplifier output again experienced excessively high noise during vibration. All leads between the tube and preamplifier were then disconnected and the vibration test repeated. The preamplifier output had excessive noise resembling the behavior of the previous two tests. It was therefore concluded that the preamplifier or the method of preamplifier mounting caused the vibration-induced noise.

Because of the inability to test the four-channel tube under vibration, a vibration test with a nine-channel tube and a permanently mounted preamplifier was planned. Because a Martin Marietta hybridized preamplifier could not be obtained to support the test, SAI designed and built a two-channel discrete preamplifier. The preamplifier components were mounted on a circuit board and the board was in turn epoxied directly to the tube header. This design resulted in very short and stiff couplings between the diode and preamplifier. The entire assembly, consisting of the tube (S/N 352) and preamplifier, was potted in an aluminum housing with Sylgard 185. The fiber optics and scintillators were not attached to the tube because of insufficient time. The light pulses from the scintillators were simulated using a LED. The S/N 352 tube had a flaw in the fiber optic faceplate that apparently developed after the glass-to-metal seal was made during tube processing. The flaw was in the form of a discoloration in the faceplate.

The S/N 352 tube discrete preamplifier and high voltage filter were tested at vibration levels of 0.1 and $0.4 \text{ g}^2/\text{Hz}$. The pretest, test and post-test counting rates at $0.4 \text{ g}^2/\text{Hz}$ are presented in Table 5. As can be noted, no apparent change in count rate occurred during vibration. The pretest, test and post-test counting rates are all within the 1σ data scatter of the counting statistics. The pulse height distributions do show a slight shift of the signal and noise. However, with the discriminator set in the valley between the signal and electrical noise, the vibration-induced signal shifts were not enough to influence the counting rate. The assembly was tested at $0.4 \text{ g}^2/\text{Hz}$ in one axis. Tests in the other axes could not be performed because after the first axis of testing, the flaw originally in the faceplate developed into a crack and caused a loss of vacuum. Post-test evaluation revealed that the flaw was originally a small fracture plane external to the

Table 5. Digicon Tube S/N 352 Vibration Test Count Rate.

TEST NO.	TEST LEVEL (g^2/Hz)	CONDITION, AXIS*	PRETEST (CPS)	TEST (CPS)	POST-TEST (CPS)	TEST TIME (SECONDS)
10	0.4	No Source, Y	5.1 ± 2.5	10.9 ± 4.4	5.7 ± 3.5	40
11	0.4	Source, Y	6793 ± 95	6802 ± 64	6759 ± 63	40
12	0.4	Source, Y	6882 ± 88	6891 ± 61	6831 ± 89	40

* Y-axis is perpendicular to tube axis and parallel to mounting plane.

vacuum envelope, and vibration testing apparently caused the fracture to grow and penetrate the seal.

Although the S/N 352 tube did lose vacuum between vibration tests, the results show that the mechanical and electrical tube design are stable at vibration levels up to $0.4 g^2/Hz$. To prevent further fracturing of the faceplate, a faceplate inspection task was incorporated into the tube manufacturing plan. Tubes with discolorations similar to S/N 352 are to be reprocessed with new faceplates.

The third Digicon tube, S/N 351, was assembled into a potential flight configuration and was vibration-tested at levels up to $0.4 g^2/Hz$. The configuration consisted of a nine-channel Digicon tube, a Martin hybridized preamplifier, fiber optics and scintillators and a high voltage filter. All components mounted on the vibration table were 'hard' mounted to the structure. No vibration isolation scheme was used in the assembly. The high voltage supply was not mounted on the vibration table. The S/N 351 tube had eight operating diodes and one diode with an open circuit internal to the tube vacuum seal.

The pretest, test, and post-test counting rates for tube S/N 351 are presented in Table 6. At vibration levels below $0.2 g^2/Hz$ no change in count rate was apparent. At $0.4 g^2/Hz$, however, vibration-induced noise was becoming apparent, causing approximately a 3.5 percent change in count rate. The pulse height distributions taken before and during $0.4 g^2/Hz$ vibration are shown in Figures 22 and 23. The distribution of Figure 22 is with the tube operating and a ^{60}CO source. It can be noted that the noise level has increased and shifted towards the discriminator setting, causing the indicated change in count rate. The distribution of Figure 23 was taken with no voltage on the tube (includes focusing voltage and diode bias) and with the preamplifier operating. Comparing Figures 22 and 23, it can be seen that the vibration-induced changes in noise level are essentially identical with or without the tube operating. From this it can be

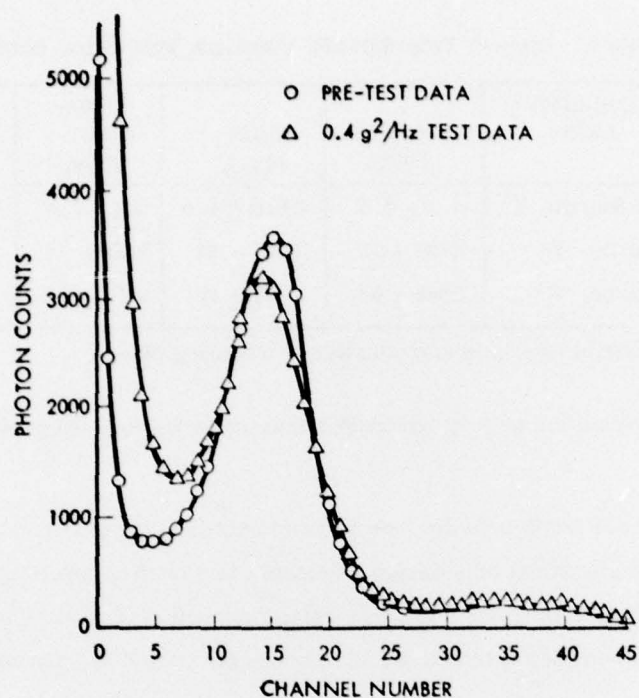


Figure 22. Sensor S/N 351 Vibration Test Pulse Height Distributions (Voltage Applied to Tube).

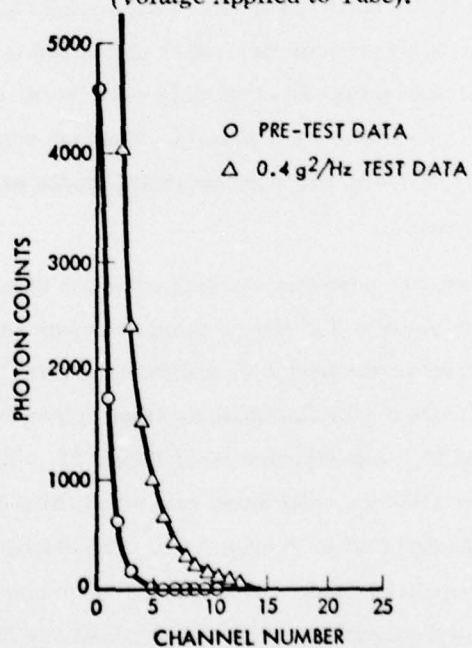


Figure 23. Sensor S/N 351 Vibration Test Pulse Height Distributions (No Voltage Applied to Tube).

Table 6. Digicon Tube S/N 351 Vibration Test Count Rate.

TEST NO.	TEST LEVEL (g ² /Hz)	CONDITION, AXIS*	PRETEST (CPS)	TEST (CPS)	POST-TEST (CPS)	TEST TIME (SECONDS)
10	0.2	No Source, Z	196 \pm 15	212 \pm 20	207 \pm 14	30
11	0.4	No Source, Z	193 \pm 15	241 \pm 22	202 \pm 19	30
11	0.4	Source, Z	6424 \pm 121	6050 \pm 141	6146 \pm 114	30
13	0.2	No Source, Y	171 \pm 16	295 \pm 17	224 \pm 18	30
13	0.2	Source, Y	6146 \pm 240	6106 \pm 116	6148 \pm 108	30
14	0.4	Source, Y	6264 \pm 134	6596 \pm 134	6256 \pm 114	30

* Y-axis is perpendicular to tube axis and parallel to mounting plane, Z-axis is tube axis.

concluded that either the preamplifier, tube header, and/or preamplifier mounting design are causing the vibration-induced noise. It may be noted that early in the vibration tests an increase in count rate was experienced in two operating vibration tests. No quantitative explanation for the increase could be found. In subsequent vibration tests the phenomenon did not reoccur.

Diagnostic tests were performed on the tube assembly, and it was concluded that the vibration sensitivity is due to the tube header/preamplifier assembly. To eliminate the vibration sensitivity, a vibration hardening task was initiated under SAMSO Contract F04701-76-C-0041, wherein tube gain increases and tube vibration isolation schemes were being investigated. Tests performed on the S/N 351 tube assembly with a preliminary vibration isolation design have shown no vibration sensitivity at 0.8 g²/Hz. The pulse height distributions taken before and during the vibration test are shown in Figure 24. Integration of the pulse height spectrum from the discriminator setting out past channel number 90 gives pretest, test and post-test counts of 35526, 35452 and 35502, respectively. As can be noted, the static and dynamic integrated counts are all within the 1 σ data scatter of the counting statistics. The pulse height distribution does not show any change during vibration. Tests at higher vibration levels were not performed. The vibration hardening task being performed under Contract F04701-76-C-0041 will be reported at a later date.

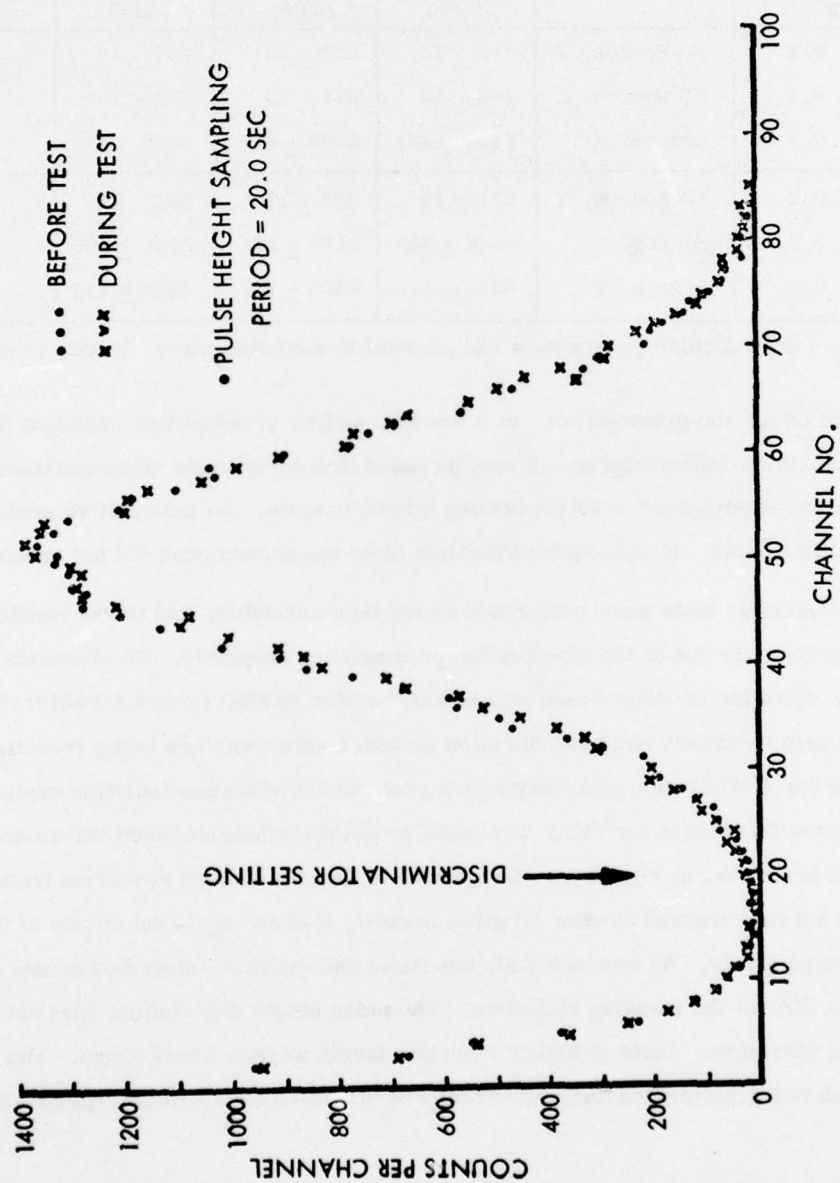


Figure 24. Pulse Height Distribution Comparison Pretest and During $0.8 \text{ g}^2/\text{Hz}$ Random Vibration.

5.0 SUMMARY AND CONCLUSIONS

A prototype multi-ray ablation sensor using a nine-channel digital photon-counting (Digicon) tube has been developed. Testing in the laboratory indicates that this multi-ray sensor has high potential for obtaining detailed shape change information on reentry vehicle nosetips during flight test.

The measured detection efficiencies of the sensor (with 0.25 inch diameter x 0.5 inch long CsI scintillator) are 35.5 percent, 26.1 percent, and 22 percent, at 0.12, 0.66 and 1.25 MeV, respectively. With a 0.25 inch diameter x 1.5 inch long CsI scintillator, the efficiency at 1.25 MeV is 50 percent. Multi-channel operation of the sensor has been demonstrated with four-channel and nine-channel prototypes. Tube-related (electrical) crosstalk is negligible (1 to 2 percent) compared to nuclear crosstalk values expected for typical multi-ray nosetip geometries. The background counting rates (~ 10 cps) are negligible relative to typical in-flight counting rates ($\sim 10,000$ cps). The projected radioactive source strength of ^{182}Ta required for a graphitic nosetip containing up to nine rays is estimated to be less than 0.1 curies. The sensor has successfully passed vibration testing at $0.8 \text{ g}^2/\text{Hz}$ with a vibration isolation system integrated into the sensor design. With no vibration isolation system (or 'hard' mounted) the sensor was found to experience approximately a 3 percent change in count rate at vibration test levels of $0.4 \text{ g}^2/\text{Hz}$. No significant change in count rate was noted with the sensor hard mounted at $0.2 \text{ g}^2/\text{Hz}$. It is therefore concluded that for the sensor to operate satisfactorily at vibration levels exceeding $0.4 \text{ g}^2/\text{Hz}$, a vibration isolation system will be required.

The principal advantages of the Digicon Multi-Ray Ablation Sensor that is continuing to be developed under SAMSO Contract F04701-76-C-0041, are as follows:

1. Compactness: A single 1.0-inch diameter x 2.0 inch long photon-counting tube, whose size is comparable to that of a single conventional space-hardened photomultiplier tube, can process light signals for up to nine gamma-ray scintillation detectors with the present diode-array design.
2. High Gamma-Ray Detection Efficiency: Unlike CdTe, the counting efficiency of the rugged CsI scintillators used in the present sensor is not limited by restrictions on the size of the crystal which can be manufactured. Efficiencies of over 50 percent have been obtained with 1.5-inch long scintillators. The high efficiency and unlimited size allows, relative to CdTe, larger collimator openings and significantly larger counting rates per unit radioactive strength.

3. Minimum Perturbation of Nosetip Packaging: Only the small, efficient scintillators (0.25 inch diameter x 1.0 inch long) and thin fiber optic bundle need be positioned in the nosetip region. The sensor and electronics, coupled to the scintillators via the flexible fiber optics, can be placed at essentially any location in the vehicle. This allows minimum perturbation in the nosetip region and provides maximum packaging flexibility.
4. Minimum Nuclear Radiation Crosstalk: The compact nature of the scintillator allows much more complete tungsten shielding both around and behind the detector, compared to other systems. Channeltron and photomultiplier tubes are attached to the scintillators and do not offer as much flexibility as the Digicon sensor in scintillator placement and shielding. CdTe requires shock isolation which restricts detector placement and occupies volume that could otherwise be used for shielding.
5. Insensitivity to Vibration: The Digicon sensor has demonstrated the ability to survive $0.4 \text{ g}^2/\text{Hz}$ and with vibration isolation is insensitive to $0.8 \text{ g}^2/\text{Hz}$ vibration levels. The inherently rugged and simple mechanical design of the Digicon tube indicates that with proper care in mounting the tube and associated preamplifier, the sensor should be quite insensitive to vibration. In addition, the sensor electronics can be easily positioned in regions of the vehicle with relatively low vibration input.
6. Unique Redundancy Capability: Several fiber optic bundles may be attached to each scintillator without sacrificing detection efficiency. Hence, by adding a second Digicon tube and using a bifurcated fiber optic coupling, the sensor reliability can be significantly enhanced.
7. Accommodates Increase in Number of Rays: Additional data channels can be added with minimal volume and Digicon tube impact.

REFERENCES

1. Orphan, V. J., et al, "Multi-Ray Ablation Sensor Development, Phase II," Report SAI-76-660-LJ, Science Applications, La Jolla, California, 7 July 1976.
2. Lisitsa, M. P., et al, Fiber Optics, Israel Program for Scientific Translations, New York, 1972.
3. Hinterberger, H. and Winston, R., "Efficient Light Coupler for Threshold Cerenkov Counters," Enrico Fermi Institute for Nuclear Studies, University of Chicago, Illinois, 1 March 1966.
4. Moody, H. L., "Test Plan for the Evaluation of the Multiple-Ray Ablation Sensor Under Simulated Reentry Vibration," Prototype Development Associates Report TR 1046-51-02, 11 December 1975.

DISTRIBUTION LIST

DEPARTMENT OF DEFENSE

Director
Defense Advanced Rsch. Proj. Agency
ATTN: Strategic Tech. Office

Defense Documentation Center
Cameron Station
12 cy ATTN: TC

Director
Defense Nuclear Agency
ATTN: TISI
ATTN: DDST
ATTN: STSP
3 cy ATTN: SPAS
3 cy ATTN: TITL

Commander
Field Command, DNA
ATTN: FCPR

Chief
Livermore Division, Field Command, DNA
Lawrence Livermore Laboratory
ATTN: FCPRL

Under Secy. of Defense for Rsch. & Engrg.
ATTN: S&SS (OS)
ATTN: AE

DEPARTMENT OF THE ARMY

Director
BMD Advanced Tech. Ctr.
ATTN: ATC-M

Program Manager
BMD Program Office
ATTN: Technology Division

Commander
BMD System Command
ATTN: BMDSC-TEB

Deputy Chief of Staff for Rsch. Dev. & Acq.
ATTN: NCB Division

Commander
Harry Diamond Laboratories
ATTN: DELHD-RC
ATTN: DELHD-RBH

Director
U.S. Army Ballistic Research Labs
ATTN: Robert E. Eichelberger

Commander
U.S. Army Mat. & Mechanics Rsch. Ctr.
ATTN: DRXMR-HH

DEPARTMENT OF THE NAVY

Chief of Naval Operations
ATTN: OP 604C4

DEPARTMENT OF THE NAVY (Continued)

Director
Naval Research Laboratory
ATTN: Code 2600, Tech. Library

Officer-in-Charge
Naval Surface Weapons Center
ATTN: Code WA-07
2 cy ATTN: Code WA-43
ATTN: C. Rowe

Director
Strategic Systems Project Office
ATTN: NSP-272

DEPARTMENT OF THE AIR FORCE

Commandant
AF Flight Dynamics Laboratory, AFSC
ATTN: FXG
ATTN: FXE
ATTN: FBC

AF Materials Laboratory, AFSC
ATTN: MBE
ATTN: MBC
ATTN: MXS
ATTN: LTM
ATTN: MXE

AF Office of Scientific Research
ATTN: Paul Thurston

AF Rocket Propulsion Laboratory, AFSC
ATTN: RTSN

AF Weapons Laboratory, AFSC
ATTN: DYV
ATTN: SUL

Headquarters
Air Force Systems Command
ATTN: DLCAM

Commander
Arnold Engineering Development Center
ATTN: XOA

Commander
Foreign Technology Division, AFSC
ATTN: PDBG

Hq. USAF/RD
ATTN: RDQSM
ATTN: RDQ

SAMSO/MN
ATTN: MNNH
ATTN: MNNR

SAMSO/RS
ATTN: RSS
7 cy ATTN: RSSE

DEPARTMENT OF ENERGY

Sandia Laboratories
ATTN: Doc. Con. for D. Rigali

DEPARTMENT OF DEFENSE CONTRACTORS

Acurex Corporation
ATTN: C. Powars
ATTN: C. Nardo
ATTN: J. Huntington

Aerojet Liquid Rocket Company
ATTN: R. Jenkins

Aerospace Corporation
ATTN: D. Geiler
ATTN: R. Mortensen
ATTN: W. Portenier
ATTN: M. Gyetvay
ATTN: H. F. Dynner
ATTN: D. T. Nowlan
ATTN: P. Legendre
ATTN: R. Hallse
ATTN: Wallis Grabowsky
ATTN: R. H. Palmer
ATTN: D. H. Platus
ATTN: W. Barry
ATTN: S. Brelant

Avco Research & Systems Group
ATTN: V. Dicristina
ATTN: John E. Stevens, J100
ATTN: William Broding
ATTN: A. Pallone
ATTN: M. Ceglowski

Battelle Memorial Institute
ATTN: Technical Library

Effects Technology, Inc.
ATTN: Robert Wengler
ATTN: A. Hunt

Fiber Materials, Inc.
ATTN: M. Subilia

Ford Aerospace & Communications Operations
ATTN: A. Demetriades
ATTN: R. Lyons

General Electric Company
Space Division
Valley Forge Space Center
ATTN: B. M. Maguire
ATTN: Phillip Cline
ATTN: D. DeBorde

General Electric Company
TEMPO-Center for Advanced Studies
ATTN: DASIAC

General Research Corporation
ATTN: Robert E. Rosenthal

Institute for Defense Analyses
ATTN: IDA Librarian, Ruth S. Smith
ATTN: Joel Bengston

DEPARTMENT OF DEFENSE CONTRACTORS (Continued)

Kaman Sciences Corporation
ATTN: Thomas Meagher
ATTN: Frank H. Shelton

Lockheed Missiles & Space Co., Inc.
ATTN: A. Mietz

Lockheed Missiles & Space Co., Inc.
2 cy ATTN: T. R. Fortune

Martin Marietta Corporation
Orlando Division
ATTN: James M. Potts, MP-61
ATTN: Laird Kinnaird

McDonnell Douglas Corporation
ATTN: L. Cohen
ATTN: H. Hurwicz
ATTN: R. Zemer

McDonnell Douglas Corporation
ATTN: W. Rinehart, Dept. 222/Bldg. 102

National Academy of Sciences
ATTN: National Materials Advisory Board for
Donald G. Groves

Physical Sciences, Inc.
ATTN: M. S. Finson

Prototype Development Associates, Inc.
ATTN: J. E. Dunn
3 cy ATTN: H. L. Moody

R&D Associates
ATTN: Paul Rausch
ATTN: Raymond F. Ross
ATTN: F. A. Field

Science Applications, Inc.
ATTN: John Warner

Science Applications, Inc.
ATTN: K. Kratsch
ATTN: Lyle Dunbar

Southern Research Institute
ATTN: C. D. Pears

Spectron Development Laboratories
ATTN: T. Lee

TRW Defense & Space Sys. Group
ATTN: W. W. Wood
ATTN: I. E. Alber, R1-1008
ATTN: D. H. Baer, R1-2136
ATTN: R. Myer
ATTN: Thomas G. Williams

TRW Defense & Space Sys. Group
San Bernardino Operations
ATTN: L. Berger
ATTN: Earl W. Allen, 520/141
ATTN: William Polich
ATTN: E. Y. Wong, 527/712
ATTN: V. Blankenship